

INFORMATION TO USERS

This manuscript has been reproduced from the microfilm master. UMI films the text directly from the original or copy submitted. Thus, some thesis and dissertation copies are in typewriter face, while others may be from any type of computer printer.

The quality of this reproduction is dependent upon the quality of the copy submitted. Broken or indistinct print, colored or poor quality illustrations and photographs, print bleedthrough, substandard margins, and improper alignment can adversely affect reproduction.

In the unlikely event that the author did not send UMI a complete manuscript and there are missing pages, these will be noted. Also, if unauthorized copyright material had to be removed, a note will indicate the deletion.

Oversize materials (e.g., maps, drawings, charts) are reproduced by sectioning the original, beginning at the upper left-hand corner and continuing from left to right in equal sections with small overlaps. Each original is also photographed in one exposure and is included in reduced form at the back of the book.

Photographs included in the original manuscript have been reproduced xerographically in this copy. Higher quality 6" x 9" black and white photographic prints are available for any photographs or illustrations appearing in this copy for an additional charge. Contact UMI directly to order.

UMI

**A Bell & Howell Information Company
300 North Zeeb Road, Ann Arbor MI 48106-1346 USA
313/761-4700 800/521-0600**

**CLIMATIC CONTROL OF THE THERMAL
REGIME OF PERMAFROST, NORTHWEST
SPITSBERGEN**

by

Jaakko Kalervo Putkonen

**A dissertation submitted in partial fulfillment of the
requirements for the degree of**

Doctor of Philosophy

University of Washington

1997

Approved by 
Chairperson of Supervisory Committee

Program Authorized
to Offer Degree _____ Geological Sciences

Date _____ 7/9/97

UMI Number: 9807016


UMI Microform 9807016
Copyright 1997, by UMI Company. All rights reserved.

**This microform edition is protected against unauthorized
copying under Title 17, United States Code.**

UMI
300 North Zeeb Road
Ann Arbor, MI 48103

Doctoral Dissertation

In presenting this dissertation in partial fulfillment of the requirements for the Doctoral degree at the University of Washington, I agree that the Library shall make its copies freely available for inspection. I further agree that extensive copying of this dissertation is allowable only for scholarly purposes, consistent with "fair use" as prescribed in the U.S. Copyright Law. Requests for copying or reproduction of this dissertation may be referred to University Microfilms, 1490 Eisenhower Place, P.O. Box 975, Ann Arbor, MI 48106, to whom the author has granted "the right to reproduce and sell (a) copies of the manuscript in microform and/or (b) printed copies of the manuscript made from microform."

Signature 
Date 8/12/97

University of Washington

Abstract

**Climatic Control of the Thermal Regime of Permafrost,
Northwest Spitsbergen**

by Jaakko Kalervo Putkonen

**Chairperson of the Supervisory Committee: Professor Bernard Hallet
Department of Geological Sciences**

The thermal link between the atmosphere and the permafrost is central to considerations of climate change consequences in Arctic areas and interpretations of deep permafrost temperatures that constitute an exceptional archive of past climate change. I studied this link by examining the principal atmospheric factors and heat transfer processes that dictate soil temperatures for an Arctic desert site in north-western Spitsbergen.

Accurate modeling of active layer temperatures requires precise treatment of thermal conduction. Unlike most models that treat soil as homogeneous with fixed thermal properties, I use realistic temporal and spatial variations in soil thermal properties based on in-situ measurements.

The heat transfer model accounted for much of the observed soil thermal regime, and it highlighted three often overlooked components of the energy budget: 1) Although air temperature is generally used as a surface boundary condition during the winter, on a daily average, the snow surface is up to 3.7°C colder than the air. 2) Heat is delivered rapidly through snow to the active layer when rain falls on snow; it infiltrates, freezes and releases latent heat near the soil surface. 3) Meltwater infiltration and freezing in the soil cause abrupt warming events and deliver nearly half of the energy to the soil in late spring. An increase in frequency or magnitude of infiltration events could mimic simple surface warming.

In view of the natural temporal variability of environmental factors, interannual changes in winter air temperature are considerably more important than other factors in changing soil temperatures, because of the duration and large temperature variability of the cold period. The latter reflects the location of the study site in an air mass boundary zone, and its response to fluctuations in air masses that have vastly different properties during the winter. Since air mass boundaries are likely to shift due to climate change, the thermal future of western Spitsbergen, Alaska and other regions situated at air mass boundary zones may be considerably more complex than simple high latitude warming, and

changes in permafrost temperatures are much more likely to reflect changes in circulation patterns than warming of any single air mass.

TABLE OF CONTENTS

List of figures.....	iii
List of Tables	v
Introduction.....	1
Background	3
Data	11
Chapter I: Active Layer Thermal Modeling	13
Modeling Soil Thermal Regime.....	13
Soil Physical Properties	14
Mineralogy, Grain Size and Regolith Thickness	15
Porosity	17
Density	20
Soil Moisture Content.....	20
Heat Capacity.....	23
Thermal Conductivity	23
Chapter II: Heat Transfer Processes in Soil.....	31
Advection of Heat due to Water Motion.....	31
Soil Internal Evaporation	32
Conduction with Phase Change, Thermal Conductivity Gradient and Unfrozen Water.....	35
Characteristic Soil Thermal Phases	40
Chapter III: Atmospheric Forcing.....	49
Summer	49
Net Radiation and Air Temperature.....	49
Winter	52
Air Temperature, Sky Temperature and Snow Surface Temperature.....	52

Air Temperature Difference Between Fjord Interior and Mouth.....	55
Snow Heat Transfer	58
Initial Density of Snow	59
Snow Metamorphism.....	60
Snow Depth.....	62
Rain on Snow	65
Chapter IV: Sensitivity of Soil Heat Flow to Current Atmospheric Variability.....	71
Spitsbergen at the Air Mass Boundary Zone	79
Chapter V: Air Mass Dynamics and Permafrost Temperatures in Alaska	86
Conclusions.....	92
List of References	99
Appendix A: Finite difference discretization.....	118

LIST OF FIGURES

<i>Number</i>	<i>Page</i>
Figure 1: Typical temperature profiles of two distinct winter air masses.	7
Figure 2: Wind direction profile of two distinct winter air masses.	8
Figure 3: The regolith depth along a nearby Kvadehuken-river.	18
Figure 4: Soil porosity as a function of depth.	19
Figure 5: Ground water depth from pore pressure transducer and manual probing.	22
Figure 6: In situ near surface (0.1 m) soil thermal conductivity and temperature.	25
Figure 7: Laboratory measurement of thermal conductivity of unfrozen/frozen soil.	26
Figure 8: Soil thermal conductivity profile for winter.	29
Figure 9: Effective heat capacity of frozen soil as a function of temperature.	37
Figure 10: Modeled and observed soil temperatures during fall freeze up 1985.	39
Figure 11: Modeled and observed soil temperatures during summer 1991..	41
Figure 12: Soil thermal conductivity profile for summer.	42
Figure 13: Modeled amount of ice in the soil during fall freeze up 1985 and thaw 1986.	44
Figure 14: Modeled and observed soil temperatures during winter 1985/1986.	46

Figure 15: Modeled and observed soil temperatures during summer thaw	
1986.	48
Figure 16: Soil heat flow 0.2 m below surface during summer 1991	50
Figure 17: The minimum difference between modeled and observed soil	
surface temperatures in a least square sense as a function of snow depth	
at the field site and temperature difference between fjord mouth and	
interior.	57
Figure 18: In situ snow depth observations at the field site and a nearby	
similar site.	64
Figure 19: Temperature at the base of the snow pack through January-	
March 1996.	68
Figure 20: Soil heat flow 0.05 m below surface during winter 1995/96	
at the field site.	69
Figure 21: Sensitivity of mean annual soil heat flow to variation in	
surface forcing.....	74
Figure 22: Winter 1985/86 sea level atmospheric pressure difference	
between White Sea and Greenland.....	82
Figure 23: Five year running mean of mean winter air temperature in	
Ny Alesund and number of winter days with steep pressure gradient.	83
Figure 24: Mean winter temperature of cold and warm air excursions.	90
Figure 25: Approximate location of Arctic air mass boundary.	91

LIST OF TABLES

<i>Number</i>	<i>Page</i>
Table 1: Physical characteristics of soil minerals.....	16

ACKNOWLEDGMENTS

The author wishes to express sincere appreciation to the following professors who contributed to this work by serving as members of my Ph D advisory Committee: chairman B. Hallet who has inspired me through these years by endless enthusiasm, E. Waddington provided constructive criticism, L. Fritschen who introduced me to micrometeorology and environmental instrumentation, L. Washburn, and S. Warren. B. Hallet, E. Waddington, and L. Washburn reviewed the dissertation; their suggestions substantially improved the presentation.

I am thankful to the following individuals who have helped make this work possible: H. Conway taught me how to program the dataloggers; T. Berg, twice assisted me in the field with amazing array of power tools; P. Berg, helped me for three months in the field and provided considerable personal support; G. Aasebostol, T.I. Karlsen and S. Thon from Norsk Polar Institute were always ready to help; M. Serreze produced the atmospheric pressure time series for Greenland and White Sea. B. Aune and I. Hanssen-Bauer provided the meteorological data pertinent to Spitsbergen. M.Fukuda conducted thermal conductivity analyses of soil samples from Spitsbergen; J. Conca measured the hydraulic conductivity of Spitsbergen soil; J. Renwick compiled the first northern hemisphere mean sea level pressure anomaly maps for me in a critical phase of theory testing. D. McTigue spent countless hours with me pondering the complications of soil

vapor transfer and how to model it; B. Bruner custom designed several electrical devices that successfully performed in harsh arctic conditions.

The following institutions helped by their co-operation and generous offers to use their infrastructure. The Norwegian Polar Research Institute provided knowledge, manpower and logistics, The Norwegian Meteorological Institute granted meteorological data, Kings Bay Coal Company helped with logistics in Ny Alesund, and Velferden allowed the use of the Geopol-hut.

This work was funded by the Academy of Finland, the National Science Foundation and the Army Research Office.

INTRODUCTION

Permafrost underlies approximately 25 % of the world's land surface, and it is widespread in high latitude and altitude regions (Judge and Pilon, 1983). The widely discussed models for contemporary greenhouse induced climate change generally predict that warming will be greatest in high latitude regions (Budyko and Izrael, 1987; Maxwell and Barrie, 1989; Roots, 1989; but see Kahl et al., 1993; Walsh, 1993; IPCC, 1996), although the warming is somewhat subdued when the effects of sulfate aerosol are included (Meehl. et al., 1996; Santer. et al., 1995). This leads to the important expectation that current and impending climate change will alter the surface energy balance, the soil temperature and, hence, the distribution of permafrost (Nelson and Anisimov, 1993; Riseborough and Smith, 1993).

The specific effects of macro scale climate change on permafrost are not likely to be simple, because of the complex nature of the interactions between climate, microclimate, surface and ground thermal conditions. Nevertheless, theoretical considerations suggest that relatively rapid changes may occur in the active layer depth, defined as the depth of summer thaw, and in the distribution of warm permafrost near its southern limit. Changes in the depth of the active layer have diverse and far-reaching implications, because all hydrologic, geomorphic, pedologic, chemical, and biological processes are sharply focused in this surface layer.

The anticipated increase in active layer depth would also have direct societal consequences; it would increase problems associated with frost heave and differential thaw settlement, which could damage and significantly increase the maintenance costs of houses, roads, airports and other structures, hinder farming (through thermokarst formation); and increase the incidence of slope stability problems (Permafrost Research, p. 15, 1983; Judge and Pilon, 1983). In addition, it may influence regions far beyond permafrost areas, because it may exacerbate greenhouse warming by releasing carbon dioxide and methane currently stored in permafrost, to the atmosphere (Oechel, 1993).

In contrast with the upper boundary of permafrost, which is defined by the depth of summer thaw, changes in the position of the lower boundary of permafrost will be generally unimportant for hundreds to thousands of years, due to the slow conductive transfer of heat over typical length scales of hundreds of meters (Osterkamp and Gosink, 1991). A virtue of this slow thermal response is that a direct archive of climatic events over the last decades and centuries lingers in permafrost temperatures.

In the presence of a changing climate, therefore, permafrost can play at least three important roles: 1) as a recorder of shallow ground temperature, stored in deep permafrost, 2) as an agent of environmental changes that affects landscapes and land-ocean and land-atmosphere interactions as well as ecological and human communities, and 3) as an amplifier of further climate change (Nelson et al., 1993).

BACKGROUND

In this work, I examine the most important factors defining the thermal regime of the soil in a permafrost area, to better understand the "complex and poorly understood regions (active layer, snow pack and boundary layer) through which the two temperatures (*permafrost and air temperature*) are coupled" (Lachenbruch and Marshall, 1986). I focus on the soil thermal processes and properties, snow and atmospheric forcing, and assess the thermal response to individual components of potential climate change on Arctic areas.

The objective is to determine the atmospheric and environmental factors (duration of snow cover, snow thickness, frequency of rain-on-snow events, air temperature during winter and summer and net radiation during summer) that control the net energy budget of high latitude soils today. This is motivated by the interest in improving the interpretation of the records of past soil temperatures, and the assessment of the effects of upcoming climate change on the thermal regime of the active layer and permafrost.

The response of the soil energy budget to changes in environmental factors depends on both heat transfer through the snow/soil system and actual changes in the character and magnitude of external climatic forcings. The former is modeled as conduction with latent heat transfers accompanying phase changes (equation 1). A measure of the latter is the

standard deviation of the atmospheric forcings for which data in the high Arctic is generally limited to the last few decades. In this work I use the observed natural variability (the standard deviation) of atmospheric forcings, as a measure of the magnitude of atmospheric changes that are likely to take place under continuing and growing anthropogenic influence (Rind and Overpeck, 1995).

Several aspects of this problem have been studied previously: including effects of snow cover on soil heat flow (Goodrich, 1974; Sturm, 1995), soil heat flow in wet arctic tundra (Osterkamp, 1995; Hinkel and Outcalt, 1994; Kane, Hinzman and Zarling, 1991), soil and snow surface heat transfer (Weller and Holmgren, 1974) and rain-on-snow events (Woo, 1981). However all researchers except Woo (1981) have focussed on relatively wet Arctic or alpine tundra areas where the soil is covered by a substantial mat of organic material. This leaves the soil thermal regime of the vast high Arctic region, which is sparsely vegetated and relatively dry, largely uncharacterized.

The work presented herein is guided by data from an Arctic desert site (latitude 78°57'29N, longitude 12°27'42E), Broeggerhalvoya in western Spitsbergen, 10 km NW from Ny Alesund, where the influence of plants, including thermal insulation and transpiration, is negligible. The relatively warm mean winter air temperature (mean of coldest month, February is -14.6°C), permits us to examine latent heat effects and other non-conductive soil heat transfer processes, that are much less evident at lower temperatures. For a description of the field site, see Hallet and Prestrud (1986).

To model the effects of upcoming climatic changes on soil thermal regime, information on potential local climatic changes is required. General Circulation Models are designed to provide this information, but currently have poor spatial resolution and different models disagree on the magnitude of upcoming changes (Tao, et al., 1996). However, the downscaling of GCM output with a coupled mesoscale model or statistical relation, seem plausible approaches in future to resolve local changes for specific areas of interest (IPCC, 1996; Russo and Zack, 1997).

The general Arctic warming predicted by GCM's is not seen in several Arctic temperature records; rather they show fluctuations of different magnitude and frequency (Pavlov, 1996; Hanssen-Bauer et al., 1990; Spencer, 1994). The lack of clear coherent warming most likely means that the large natural variability of the Arctic climate system is obscuring the anthropogenically induced global warming, at least locally (Russo and Zack, 1997). The lesser than expected warming can also partly be explained by cooling due to sulfate aerosols (Meehl, et al., 1996; Santer, et al., 1995). Alternatively, the response to anthropogenic influence may be spatially complex with some regions cooling while others warm, which would be consistent with observed circum-Arctic changes in air temperature over the last thirty years (Chapman and Walsh, 1993).

I begin by developing a thermal model of soil surface heat flow under atmospheric forcing. This model is tested, validated and calibrated using soil temperature and

micrometeorological data from a field site in western Spitsbergen. Then, the sensitivity of the soil heat flow to individual primary components of atmospheric forcing is examined. Existing meteorological data sets are studied to establish the natural variability of primary atmospheric forcings. A variety of boundary conditions for the soil heat flow model are then introduced sequentially to represent each atmospheric forcing perturbed from its reference value by the magnitude of its standard deviation. Finally, the resulting soil heat flow perturbations, caused by specific atmospheric forcing perturbations are compared to one another. It is shown that, relative to other atmospheric changes, year to year variations in winter (defined herein as the snow cover period, generally from December to May) air temperature, have the greatest impact on soil heat flow under current climatic conditions.

The particular climatic characteristics of this field area and their effect on permafrost temperatures, are also worth introducing at this point, to motivate further the research. In western Spitsbergen, the winter is commonly punctuated by warm intervals during which moist, warm Atlantic (Figures: 1 and 2) air sweeps over the area. This air mass produces heavy snow, slush and rain as it converges with cold Arctic air. Liquid water delivered to the snow surface, percolates through the snow pack and freezes at the soil surface. These events are important because significant energy can be delivered to the base of the snowpack, and hence, confound the correlation between the air temperature and the temperature of the soil surface and permafrost. However, they are largely undetectable in

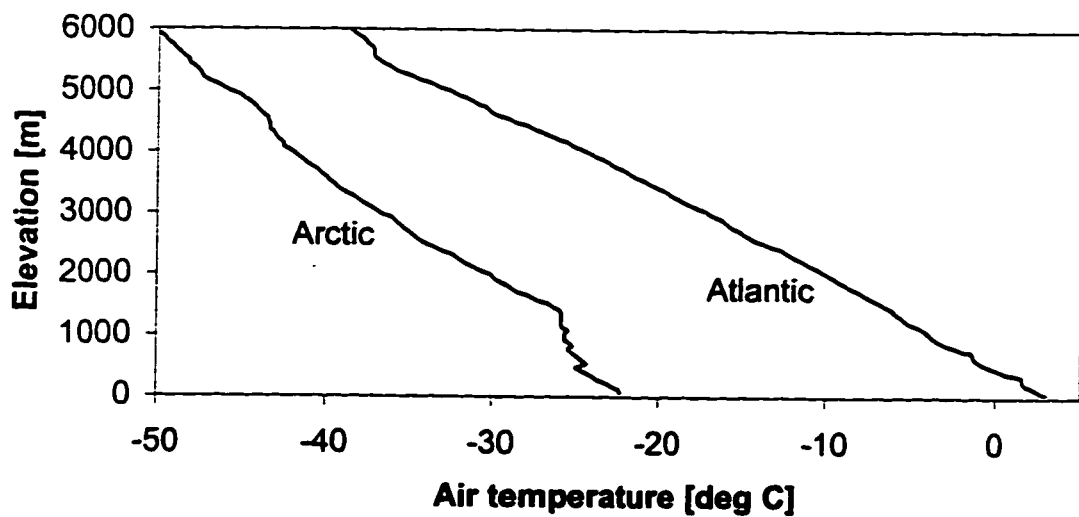


Figure 1: Typical temperature profiles of the two distinct winter air masses, Arctic (12/26/95), and Atlantic (3/12/96) that pass over Spitsbergen. They were measured 10 km from the field area, at the Alfred Wegener Institute research station in Ny Alesund. The Atlantic air mass is as much as 20°C warmer and even exceeds the freezing point close to surface; the downward long wave radiation is increased as well.

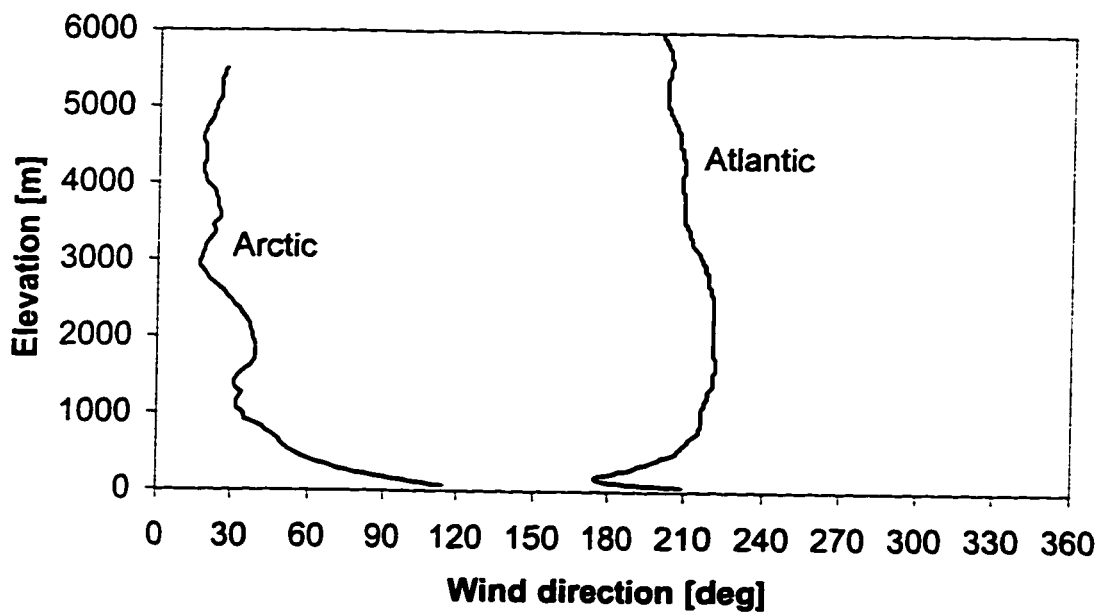


Figure 2: Winter wind direction (facing upwind) profiles corresponding to Figure 1 data show that warm air originates over the North Atlantic, and cold air over Arctic Ocean.

air temperature records, because the increase in air temperature up to the freezing point is not correlated with the amount of precipitation.

A further advantage of studying soil/atmosphere energy exchange in Spitsbergen is that it is situated within the major pathway of atmospheric energy flux into the arctic basin (Overland and Turet, 1994), and the ocean surrounding the island group is the locus of the main ocean currents that circulate arctic ocean waters. Therefore, as the ramifications of climate change are predicted to be largest in the Arctic, this principal energy pathway would be potentially a prime area to detect past and present climatic changes and their effect on permafrost.

The work published here is consistent with the philosophy of modern interdisciplinary Arctic system research, in which a range of spatial scales are considered in studies from the square meter level processes to continental scale climate dynamics (Arctic System Science, Land Atmosphere Ice Interactions long range plan: ARCCS LAII, 1996). It is also guided by the recommendation of the Intergovernmental Panel on Climate Change (IPCC, 1990) to direct research toward understanding the physical relationship between permafrost temperatures and air temperatures.

The first three chapters focus on measurements and analysis of thermal processes in the active layer and the energy linkage between the atmosphere and the soil. I then examine several issues:

- whether vapor advection and associated phase changes in the soil are important heat transfer processes during the summer and fall freeze up at this site, as suggested by Hinkel and Outcalt (1994) based on their studies in Alaska
- how modeling of heat conduction is affected by using field-monitored spatial and temporal variation in soil thermal properties due to variations in moisture content and phase changes
- how soil thermal forcing during summer is dominated by air temperature and net radiation, and hence is directly and distinctly affected by cloudiness
- how winter air temperature (commonly used as a surrogate for snow surface temperature) is distinct, but related to snow surface temperature and to radiative sky temperature
- how soil temperatures are affected by rain-on-snow events

The last two chapters (IV and V) explore the relative contribution of diverse environmental factors (snow depth, frequency of rain-on-snow events, air temperature during winter and summer and net radiation during summer) to the soil thermal regime. Changes in soil heat flux in Spitsbergen are shown to depend sensitively on the frequency with which air masses with contrasting properties pass over Spitsbergen. The connection between air mass dynamics and soil heat flux is examined comparatively for Spitsbergen and North America. I suggest that deep permafrost temperatures that have been obtained from air mass boundary areas in Alaska and Canada are probably more sensitive reflectors of past air mass dynamics than changing temperature of any air mass.

DATA

A program of automated soil temperature recordings was initiated in the summer of 1984, at a patterned ground field site described by Hallet and Prestrud (1986). Thermistors were placed approximately 0.1 m apart in an epoxy-filled PVC rod (18 mm outside diameter), buried in the center of a fine-grained domain of a sorted circle, down to 1.14 m below the ground surface. The thermistors were linked to a digital microprocessor; the frequency of measurements varied from 1-24/day. The resolution of the thermistors is 0.004°C, and the accuracy is estimated to be 0.02°C near 0°C. Complementary recordings of frost heave and pore pressure were also available. Soil samples were collected to determine their mineralogy, moisture content, thermal and hydraulic conductivity, and bulk density in the laboratory. During the 1991 summer additional sensors were installed: two soil heat flow transducers (Radiation and Energy Balance Systems, Inc. (REBS), HFT-3, accuracy 0.1 W m⁻², 0.1 m and 0.2 m below surface), a net radiation sensor (REBS, model Q*6, accuracy 0.1 W m⁻²), anemometer, rain gauge, and humidity and air temperature sensors (Campbell Scientific Inc, Model 207). In addition, a thermal conductivity probe was installed 0.1 m below surface (Soiltronics, model TC2, accuracy ± 5 % (Shiozawa and Campbell, 1990)).

Additional atmospheric data were obtained from the research station in Ny Alesund, located within 10 km of the study site. They include a complete surface radiation budget

through the study period (Hisdal, Finnekasa and Vinje, 1992), standard meteorological records (I. Hanssen-Bauer and B. Aune, Norwegian Meteorological Institute pers. comm., 1992; Hanssen-Bauer, Kristensen Solas and Steffensen, 1990), and upper air soundings (0-30 km) for temperature and wind direction profiles (Koenig-Langlo and Marx, 1997).

Three relatively uninterrupted periods of data were used in the analyses: one year beginning in September 1985 to model a complete annual cycle, and the 1991 and 1992 summers to examine more closely higher frequency events and their relation to atmospheric forcing. In light of standard meteorological observations, the September 1985-August 1986 period, was average. Mean annual air temperature was -6.6°C , 0.4°C colder than the long term (1975-1990) mean, but well within the mean variability ($\sigma = 1.3^{\circ}\text{C}$). Annual precipitation was 17 % larger than long term mean (372 mm), however the number of rain-on-snow events was less (3) than average (5.5). During the 1991 summer, the mean air temperature for July-August in Ny Alesund was 4.7°C , which is 0.2°C colder than the long-term mean. Overall, the reference periods are close to long-term averages.

CHAPTER I: ACTIVE LAYER THERMAL MODELING

MODELING SOIL THERMAL REGIME

Much insight into the thermal regime of a laterally uniform soil can be gained using the general one-dimensional thermal diffusion equation with phase change (1).

$$\rho c \frac{\partial T}{\partial t} = \frac{\partial \left(k \frac{\partial T}{\partial z} \right)}{\partial z} + \frac{L_f \rho_w \partial V_f}{V_u \partial t} = \frac{\partial k \partial T}{\partial z \partial z} + k \frac{\partial^2 T}{\partial z^2} + \frac{L_f \rho_w \partial V_f}{V_u \partial t} \quad (1)$$

Where T is temperature [$^{\circ}\text{C}$], t is time [s], ρc is the soil heat capacity [$\text{J m}^{-3} \text{K}^{-1}$], k is soil thermal conductivity [$\text{W m}^{-1} \text{K}^{-1}$], z is depth [m], V_u is unit volume [1 m^3], L_f is latent heat of fusion of ice [J kg^{-1}], ρ_w is density of water [kg m^{-3}], V_f is volume of ice [m^3].

Physically this means that the time rate of temperature change is related to thermal conductivity and temperature gradient both above and below the level of interest and the rate of ice formation within the soil. The term for ice formation integrates both phase change at 0°C and the progressive freezing of unfrozen water as temperatures decrease below 0°C .

Measured soil temperatures were compared to temperatures calculated using an explicit finite difference approximation of equation (1) with two boundary conditions (for details of the discretization process see appendix A): the measured surface temperature and the temperature at 15 m, which was assumed fixed at -4.0°C . This basal temperature is the mean annual soil temperature at the lowest measurement level (1.14 m) corrected by 0.375°C to account for the geothermal gradient (using an average continental geothermal gradient of $25^{\circ}\text{C} / 1000 \text{ m}$ for 14 m). This 15 m temperature corresponds closely to measurements obtained in comparable settings elsewhere in Spitsbergen. These borehole measurements in Ny Alesund, Longyearbyen and Svea Gruva reveal temperatures between -3 to -7°C at 10-20 m (Liestol, 1975; Gregersen and Eidsmoen, 1988). The depth to bedrock and the thermal properties of bedrock are estimated from observations and from analyzed samples (see sections below).

SOIL PHYSICAL PROPERTIES

Quantitative consideration of the soil thermal regime requires the heat capacity and thermal conductivity of the soil to be specified realistically. These thermal parameters depend on soil mineralogy, porosity and moisture content, as summarized in Table 1. These parameters commonly vary with depth and time because they are related to soil moisture content that also tends to vary in natural soils. Therefore, detailed thermal analysis essentially requires continuous in situ measurements of thermal properties.

MINERALOGY, GRAIN SIZE AND REGOLITH THICKNESS

The soil, comprising much of the fine-grained centers of sorted circles where the temperature data of interest were obtained, is a silt loam (Mann, Sletten and Ugolini, 1986). It contains considerable gravel, averaging 58.5 % by weight, and ranging from 23-82 % (pers. comm. B.Hallet, 1995). Mineralogically, the soil resembles the underlying bedrock and consists mainly of dolomite (80 %) and quartz, with varying amounts of feldspars and mica (Etzelmuller and Sollid, 1991). The gravel (particles 0.5 to 5 cm in

Table 1: Physical characteristics of soil minerals.

Mineral Type	Mineral Density ⁽¹⁾ [kg m ⁻³]	Volume Fraction	Heat Capacity ⁽²⁾ [J kg ⁻¹ K ⁻¹]	Thermal Conductivity [W m ⁻¹ K ⁻¹] ⁽¹⁾⁽²⁾
Dolomite	2830	0.8	813	4.98
Calcite	2700	0.1	795	3.66
Quartz	2650	0.1	700	8.09

⁽¹⁾Clark (1966)

⁽²⁾Berman and Brown (1985)

diameter), which is abundant even in the fine-grained soils is dominantly comprised of carbonates (up to 83 %), mostly dolomite with some calcite (Mann, Sletten and Ugolini, 1986). In this work the following representative mineralogy is used for the soil: 80 % dolomite, 10 % calcite, and 10 % quartz by volume.

The mean depth of the regolith at the field site is estimated to be 1.4 ± 0.2 m, based on hand probing at the site in the late summer and examining soil stratigraphy at representative cross sections along the nearby Kvadehuken-river (Figure 3), which show relatively thick regolith on major former beach ridges (Tolgensbakk & Sollid, 1987) and thinner cover in swales between them. The field site is located in such an inter beach-ridge swale. The regolith thickness corresponds approximately with the active layer depth.

POROSITY

Calculations of porosity are based on two sets of soil samples taken simultaneously from one excavation in sorted circle fines (8/6/85, S. Prestrud-Anderson). Samples were obtained from four different levels (0, 0.2, 0.4, and 0.6 m below surface) for bulk density and moisture content analyses (Figure 4). For each level porosity was calculated from mean values of each data set. Uncertainty limits represent the combination of standard deviation of bulk density and moisture content. There appears to be slight increase in porosity towards surface, but as it is well within uncertainty limits the whole section is assigned one representative porosity value: 0.26 ± 0.03 . A few spot Time Domain

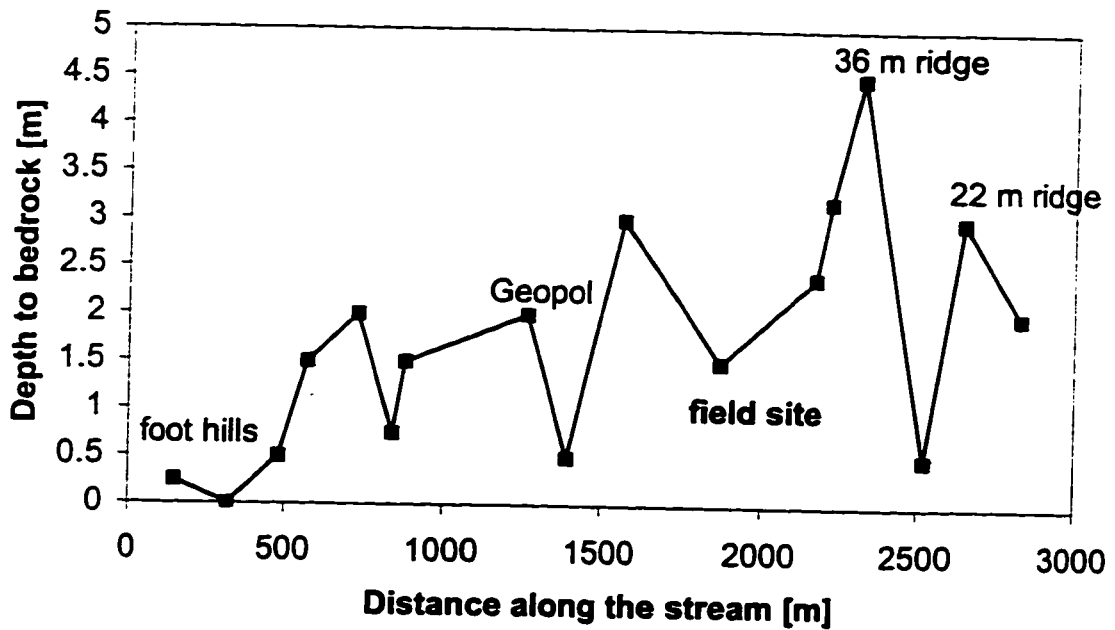


Figure 3: Regolith thickness along the Kvadehuken river that cuts across elevated beach ridges near the field site. The thickness is greatest on beach ridges and thinnest in intervening swales. The field site is located in such a swale, where the regolith, as well as the active layer depth averages 1.4 ± 0.2 m in depth, based on late summer hand probing.

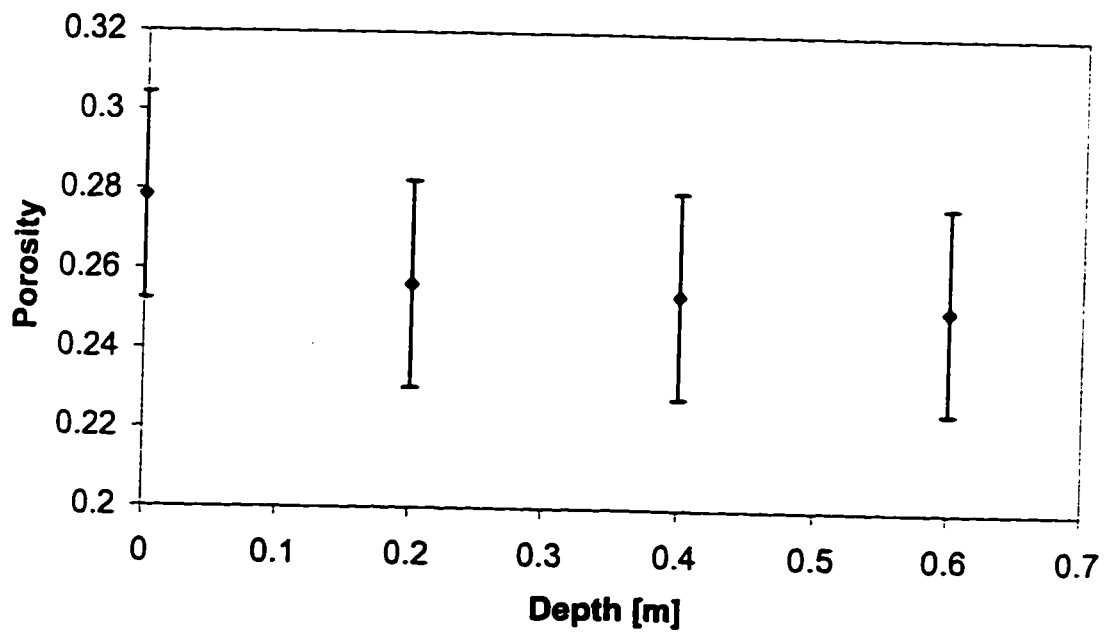


Figure 4: Mean soil porosity as a function of depth, based on two sets of soil samples collected by S. Prestrud-Anderson on August 6, 1985 for bulk density and moisture content analyses. Uncertainty limits represent extreme combinations of bulk density and moisture content (each within one standard deviation of the mean).

Reflectometry (TDR)-measurements (Hydra Probe, Vitel Inc.) at the field site, when the soil was saturated, gave an average porosity of 0.29 ± 0.03 , from the surface to a depth of 0.5 m, which corresponds well with the 0.26 value used throughout this work, when uncertainties are taken into account. The temporal evolution of soil moisture content is described below.

DENSITY

The soil bulk density is dictated by the porosity, moisture content and densities of constituent minerals (Table 1). The average of the mineral densities, weighted according to their volume fractions, is 2800 kg m^{-3} . The corresponding bulk densities of dry and water-saturated soil are 2070 kg m^{-3} and 2330 kg m^{-3} , using a porosity of 0.26.

SOIL MOISTURE CONTENT

The field site is located a few tens of meters from a small lake on an essentially horizontal surface, and hence remains moist throughout the summer. A pore pressure transducer, that reflects the height of the free water column, was installed 0.55 m below the soil surface within the saturated soil domain. Depth to ground water table was also measured in a ground water tube, inserted 10 m from the site. These point measurements are generally consistent with the continuous pore pressure data. The variation of the ground water table depth during most of July and August 1991, which is the period of intensive modeling, is of the order of the vertical resolution of the thermal model and is therefore assigned a representative mean value 0.4 m.

Above the ground water table the fine grained soil is unsaturated, but still contains considerable capillary water. The unsaturated soil moisture content at level of 0.2 m below surface was obtained by sampling the site weekly through the thaw season and determining the volumetric moisture content in the lab; the mean for the summer was 0.21 ($\sigma = 0.02$). This unsaturated soil moisture content is close to the moisture content expected based on the soil moisture retention capacity estimated from the soil particle size distribution and the distance to water table, as shown by van Genuchten (1976). In conclusion, the soil moisture content at this study site does not vary appreciably during the course of the summer, after the initial thaw at the beginning of July (Figure 5).

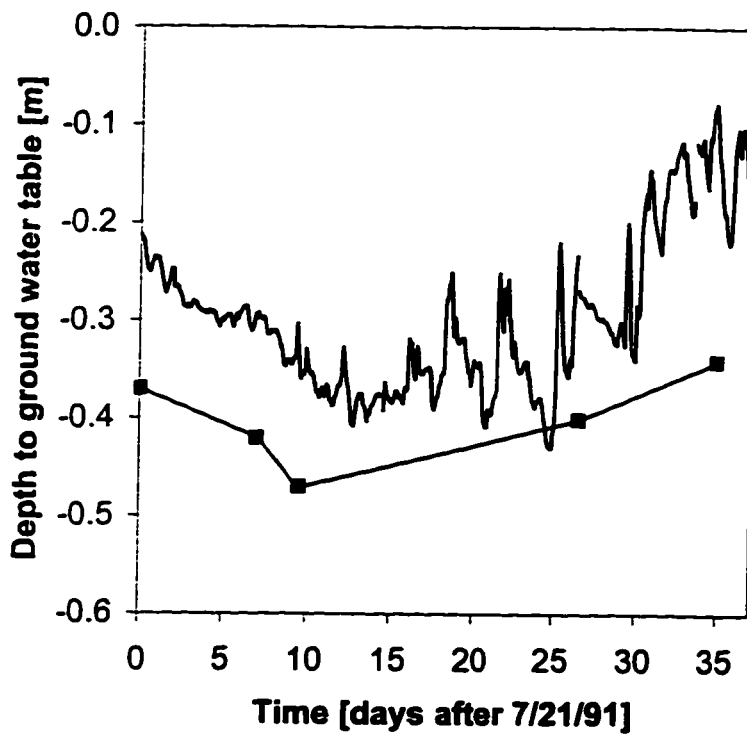


Figure 5: Position of ground water table from pore pressure transducer and manual probing. The probed depth is measured about 10 m away and upslope from pore pressure transducer, which may account for the difference between data sets. In the model, the mean depth of 0.4 m was used from the end of July through August 1991.

HEAT CAPACITY

The heat capacity of the mineral phase is $800.5 \text{ J kg}^{-1} \text{ K}^{-1}$, based on the heat capacity of the primary minerals and their mass fractions (Berman and Brown, 1985), (Table 1). The corresponding bulk soil volumetric heat capacities (ρc) range from $2.72 \cdot 10^6 \text{ J m}^{-3} \text{ K}^{-1}$ for saturated soils to $1.68 \cdot 10^6 \text{ J m}^{-3} \text{ K}^{-1}$ for dry soils. The heat capacity in the summer modeling reflects the observed soil moisture content.

For the winter period there is no independent measurement of the frozen soil heat capacities and of the distribution of ice, voids and mineral material. However, as the ratio of the heat capacities of ice to mineral matter is close to unity (0.93), the heat capacity is insensitive to variation in ice or mineral fraction. (In contrast, in summer the corresponding ratio of water to mineral matter is 1.87.) Consequently, in winter the heat capacity for the entire soil profile is assigned one representative value $2.1 \cdot 10^6 \text{ J m}^{-3} \text{ K}^{-1}$. The heat capacities of mineral material ($2.24 \cdot 10^6 \text{ J m}^{-3} \text{ K}^{-1}$) and ice ($2.1 \cdot 10^6 \text{ J m}^{-3} \text{ K}^{-1}$) are both within 7 % of the suggested mean value. A small volumetric fraction of voids (~6 %) in the soil will reduce the heat capacity to $\sim 2.1 \cdot 10^6 \text{ J m}^{-3} \text{ K}^{-1}$.

THERMAL CONDUCTIVITY

The thermal conductivity of the mineral fraction can be estimated closely (Sass, Lachenbruch and Munroe, 1971) from the geometric mean of the conductivities of the individual mineral constituents (see Table 1):

$$k_{\text{solid}} = (k_{\text{Dolomite}})^{0.8} (k_{\text{Calcite}})^{0.1} (k_{\text{Quartz}})^{0.1} = 5.0 \text{ W m}^{-1} \text{ K}^{-1} \quad (2)$$

The thermal conductivity of nearsurface (0.1 m depth) unsaturated soil was also measured by a needle probe (Shiozawa and Campbell, 1990), activated once a day to provide an in situ measurement during the 2/26/95-7/21/96 period (Figure 6). The probe heats the soil for a short time period and simultaneously monitors the transient temperature, which is a function of thermal conductivity of the surrounding material (Shiozawa and Campbell, 1990). The mean unfrozen and frozen thermal conductivities for this period are respectively $2.8 \text{ W m}^{-1} \text{ K}^{-1}$ and $3.0 \text{ W m}^{-1} \text{ K}^{-1}$; standard deviations are respectively $0.19 \text{ W m}^{-1} \text{ K}^{-1}$ (6.9 %) and $0.16 \text{ W m}^{-1} \text{ K}^{-1}$ (5.6 %), which correspond well with the reported (± 5 %) accuracy of the probe (Shiozawa and Campbell, 1990). The measurements of the thermal conductivity of unfrozen soil compare favorably with $2.7 \text{ W m}^{-1} \text{ K}^{-1}$ value (0.26 porosity and 0.21 moisture content), calculated using an empirical relation suggested by Johansen (1975). Laboratory measurements with saturated soil sample from the field site yielded $2.7 \text{ W m}^{-1} \text{ K}^{-1}$ ($\sigma = 0.04 \text{ W m}^{-1} \text{ K}^{-1}$, 1.6 %) for unfrozen soil ($\sim 20^\circ\text{C}$, porosity 0.30 ± 0.03) $3.9 \text{ W m}^{-1} \text{ K}^{-1}$ ($\sigma = 0.32 \text{ W m}^{-1} \text{ K}^{-1}$, 8.2 %) for frozen soil at -15°C (Figure 7). Similar measurements with a field site sample by M. Fukuda (pers. comm. 1993), yielded values for saturated sample; -20°C , $4.5 \text{ W m}^{-1} \text{ K}^{-1}$ and 20°C , $2.6 \text{ W m}^{-1} \text{ K}^{-1}$, which generally agree with other data presented here. These numbers are

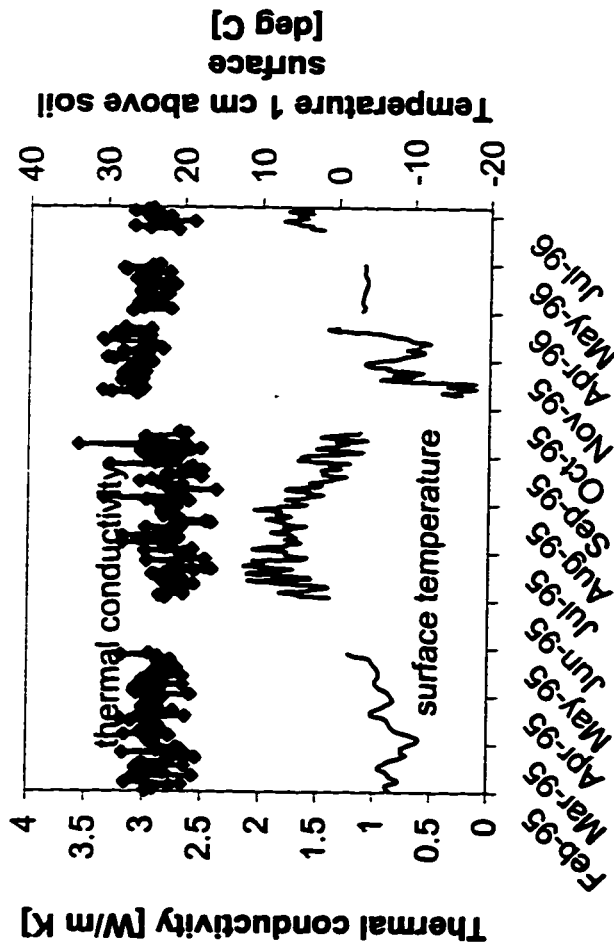


Figure 6: In situ near surface (0.1 m) soil thermal conductivity measured with a needle probe, and temperature during the winter 1995 and summer 1996; note discontinuous time scale. The mean thermal conductivities for unfrozen and frozen soil for this period are respectively $2.8 \text{ W m}^{-1} \text{ K}^{-1}$ and $3.0 \text{ W m}^{-1} \text{ K}^{-1}$. These differ significantly from laboratory measurements suggesting that the soil structure in remolded laboratory samples differs substantially from that in the field.

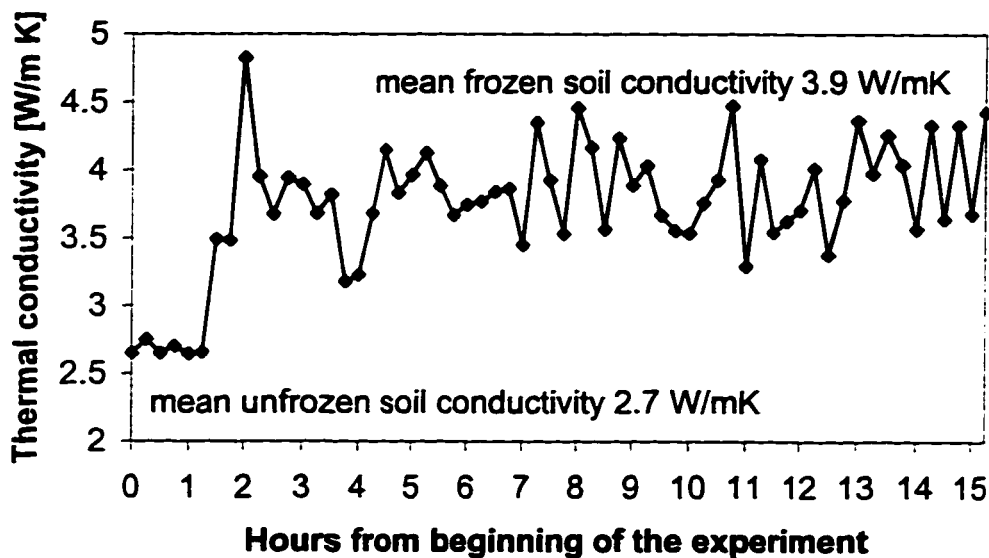


Figure 7: Laboratory measurements of thermal conductivity of a saturated fine grained soil sample from the field site yielded average $2.7 \text{ W m}^{-1} \text{ K}^{-1}$ (standard deviation: $0.04 \text{ W m}^{-1} \text{ K}^{-1}$) in the unfrozen ($\sim 20^\circ\text{C}$, porosity 0.30 ± 0.03) and $3.9 \text{ W m}^{-1} \text{ K}^{-1}$ (-15°C , standard deviation: $0.32 \text{ W m}^{-1} \text{ K}^{-1}$) in the frozen state. The frozen 10^3 cm^3 sample was completely frozen in one hour. The rapid freezing and observed lack of ice lensing are probably responsible for the conductivity of the frozen sample being considerably higher than that measured in situ (Figure 6).

similar to the geometric mean (equation (2)) of respective conductivities of saturated soil (frozen $4.0 \text{ W m}^{-1} \text{ K}^{-1}$ and unfrozen $2.8 \text{ W m}^{-1} \text{ K}^{-1}$). However, the field measurements are deemed most representative, because the lab samples may have quite unrealistic soil structure and ice lens characteristics, which can affect the conductivity considerably (Hallet and Rasmussen, 1993). The large difference between laboratory and in situ measured thermal conductivity for frozen soil, suggests that in situ frozen soil near the ground surface contains air voids, lowering the thermal conductivity there. These are presumably formed in close connection with pervasive ice lensing within the soil structure (Hallet and Rasmussen, 1993).

I determined the soil thermal conductivity from temperature data for 0.1 m depth for winter 1985/86 frozen ground, because no direct thermal conductivity measurements were available for the period and location of interest. With equation (1) and observed soil temperatures at two different levels within the uppermost 0.2 m as boundary conditions. The thermal conductivity was allowed to vary to find the effective thermal conductivity ($2.0 \text{ W m}^{-1} \text{ K}^{-1}$) in a least square sense that best reproduced the observed temperatures in the level between the two boundary temperatures.

To determine whether the conductivity varies significantly with depth due to vertical variation in moisture content or textural characteristics, I examined periods when the time rate of temperature change at each model grid level vanishes ($dT/dt = 0$) in equation (1). For this to occur the divergence of the heat flux also has to vanish, which implies that:

$$k_1 \left(\frac{\partial T}{\partial z} \right)_1 = k_2 \left(\frac{\partial T}{\partial z} \right)_2 \quad (3)$$

where k_1 and k_2 are the thermal conductivities [$\text{W m}^{-1} \text{K}^{-1}$] of upper and lower control volumes respectively.

Thus (3) can be solved for the ratio of conductivities, and a complete conductivity profile can be obtained based on the independently measured surface conductivity (Figure 8). A twofold increase in the thermal conductivity occurs between the surface and 1.2 m depth, presumably due to a decrease in void fraction and changes in texture and ice content with depth.

The conductivity profile is defined for a period with no rain-on-snow events and when soil temperatures were sufficiently low ($\sim 10^\circ\text{C}$) to prevent complications caused by unfrozen water (as discussed below). This period was also chosen to include only temperature changes that were slow. If the soil temperatures were fluctuating rapidly, periods of vanishing dT/dt (as required when using equation (3)) would be rare and short lived, and the intermittent sampling could miss temperature peaks and hence misrepresent the mean thermal forcing during that period.

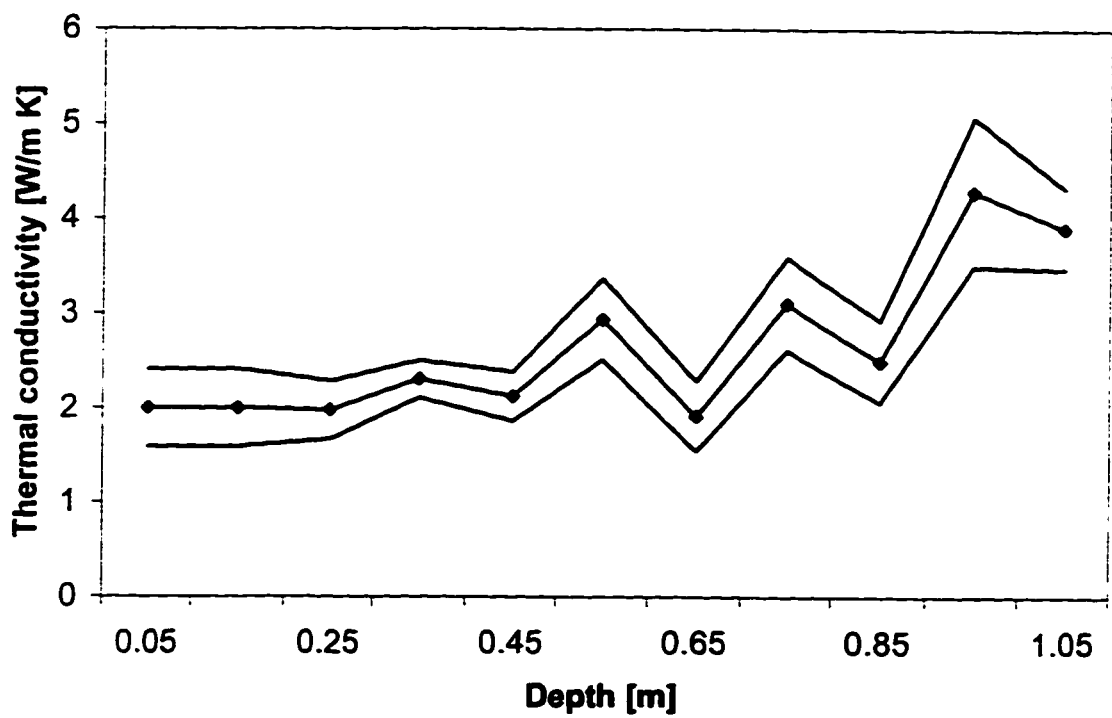


Figure 8: Vertical thermal conductivity profile for the winter obtained from the temperature data (see text). Uncertainty limits of one standard deviation are also shown.

This method of determining the soil vertical conductivity profile is based on assumptions that: 1) conduction is the primary heat transfer process in the soil during this period, and no latent heat effects are present (for justification see Chapter II, Soil Internal Evaporation), 2) heat flow is strictly one-dimensional and in the vertical direction. Failure of these assumptions would undermine the calculated conductivities. Additional errors could arise from the finite accuracy of the soil temperature measurements; however, these are likely to be minor because the typical temperature difference between adjacent thermistors is about an order of magnitude larger than the accuracy of the system (0.02°C).

CHAPTER II: HEAT TRANSFER PROCESSES IN SOIL

Studies of the thermal behavior of arctic soils have suggested that vapor advection and associated latent heat effects may significantly contribute to the heat transfer in unfrozen soils. Herein, I examine the heat transfer through both general calculations based on widely accepted theory on soil mass and energy flow (Philip and de Vries, 1957) and thermal modeling based on field measurements of soil temperatures.

ADVECTION OF HEAT DUE TO WATER MOTION

In addition to heat conduction, which always occurs when the temperature gradient and conductivity are both finite, heat advection due to pore fluid migration can be significant. Thermal effects of fluid flow in porous medium can be assessed by calculating the Peclet number that is a ratio between advective and conductive heat transfer (equation 4). To maximize advection effects, I consider the most rapid flow velocity likely to occur naturally in the soil from the study site: the vertical velocity in a freely draining saturated soil. This water velocity ($u = 1.35 \cdot 10^{-8} \text{ m s}^{-1}$) was determined from the hydraulic conductivity obtained by centrifuge method (pers. comm, J. Conca, 1993). Any rapid water flow is likely to be confined to the active layer, hence the active layer depth ($\sim 1.5 \text{ m}$) can be used for the characteristic length in the Peclet number:

$$Pe = \frac{uL}{\kappa} = 6.7 \cdot 10^{-3}$$

(4)

where κ is representative bulk soil thermal diffusivity = $1 \cdot 10^{-6} \text{ m}^2 \text{ s}^{-1}$.

The Peclet number ($2 \cdot 10^{-2}$) is much less than one, which suggests that heat advection due to water flow is negligible. Similar results have been reported from Taimyr, Siberia (Boike et al., 1997).

During freeze up both the volumetric expansion of water due to freezing and ice lensing tend to break the soil structure and reduce the hydraulic conductivity, allowing more rapid infiltration once the soil thaws. However, the frost-induced increase in soil hydraulic conductivity is generally less than an order of magnitude (Chamberlain and Gow, 1979) and, hence, advection is still very likely to be unimportant because the Peclet number is still much less than unity.

SOIL INTERNAL EVAPORATION

The importance of internal evaporation and condensation in the active layer, which has been stressed by Hinkel et al. (1990); Hinkel and Outcalt (1993); Hinkel and Outcalt (1994), can be assessed through the physically based coupled energy and mass transfer model, formulated originally by Philip and de Vries (1957), modified by Milly (1982, 1984) and applied more recently by Scanlon and Milly (1994).

Vapor flux is governed by two relations:

$$q_{\text{thermal vapor}} = D_{\text{thermal vapor}} \frac{dT}{dz}$$

and

$$q_{\text{isothermal vapor}} = D_{\text{isothermal vapor}} \frac{d\psi}{dz}$$

Where: $q_{\text{thermal vapor}}$ is mass flux of vapor due to a thermal gradient [ms^{-1}], $D_{\text{thermal vapor}}$ is vapor conductivity associated with a temperature gradient [$\text{m}^2 \text{ s}^{-1} \text{ K}^{-1}$], $q_{\text{isothermal vapor}}$ is mass flux of vapor due to a pressure head gradient [m s^{-1}], $D_{\text{isothermal vapor}}$ is isothermal vapor conductivity [m s^{-1}], ψ is pressure head [m].

Both conductivities depend on temperature, soil moisture content and grain size distribution. To obtain a liberal order of magnitude estimate of the vapor flux, a soil temperature of 25°C is assumed (actual soils are colder, and hence would have lower conductivities). In terms of soil moisture content, both conductivities peak in relatively dry soil. The highest conductivities found by Milly (1994) for two soils of interest (silty clay and loamy sand, which are similar to the study site soil: silt loam being slightly finer and the other slightly coarser) are: $D_{\text{thermal vapor}} = 3 \cdot 10^{-11} \text{ m}^2 \text{ s}^{-1} \text{ K}^{-1}$ and $D_{\text{isothermal vapor}} = 1 \cdot 10^{-14} \text{ m s}^{-1}$. The corresponding maximal vapor flux is:

$$q_{\text{thermal vapor}} = -3 \cdot 10^{-11} \text{ m}^2 \text{ s}^{-1} \text{ K}^{-1} (dT/dz)$$

and corresponding latent heat flux in soil is:

$$q_{\text{thermal vapor}} \rho_{\text{water}} L_e (dT/dz) = 0.075 \text{ W m}^{-1} \text{ K}^{-1} (dT/dz)$$

where: L_e is energy of evaporation = $2.5 \cdot 10^6 \text{ J kg}^{-1}$. This vapor flux is directed from warm to colder domains. The maximum potential heat transfer contribution of thermal vapor flux is equivalent to an effective 3 % increase in characteristic thermal conductivity ($3 \text{ W m}^{-1} \text{ K}^{-1}$).

The maximum isothermal vapor flux due to a pressure head gradient is calculated using the $D_{\text{isothermal vapor}}$ ($1 \cdot 10^{-14} \text{ m s}^{-1}$) and the maximum assumed pressure head gradient. The pressure head of very fine grained surface soil is on the order of $-1.5 \cdot 10^6 \text{ Pa}$ (pers. comm. R. Sletten, 1996); with water saturated soil at 1 m depth and such dry soil at the surface, the pressure head gradient would be only 150 which is less than liberal order of magnitude estimate (10^3) used here for pressure head gradient:

$$q_{\text{isothermal vapor}} = 1 \cdot 10^{-14} \text{ m s}^{-1} 10^3 = 1 \cdot 10^{-11} \text{ m s}^{-1}$$

The corresponding latent heat transfer to the site of evaporation is:

$$q_{\text{isothermal vapor}} = \rho_{\text{water}} L_e =$$

$$1 \cdot 10^{-11} \text{ m s}^{-1} 10^3 \text{ kg m}^{-3} 2.5 \cdot 10^6 \text{ J kg}^{-1} = 0.025 \text{ W m}^{-2}$$

Typical conductive soil heat fluxes exceed this latent heat transfer associated with vapor transport and condensation by more than two orders of magnitude; hence, thermal behavior is for all practical purposes purely conductive. Other potential mechanisms to drive significant heat transfer in soil, such as chemically induced free energy gradients (Kane and Hinkel, 1994), have yet to be documented.

CONDUCTION WITH PHASE CHANGE, THERMAL CONDUCTIVITY GRADIENT AND UNFROZEN WATER

In this section, I introduce processes and phenomena that Figure importantly in but complicate the soil thermal analysis; these are commonly omitted from soil thermal models.

Thermal properties of natural soils do vary vertically due to changes in texture, lithology, moisture and/or organic content (Woo and Xia, 1996). The general thermal conduction equation (1), contains a term explicitly accounting for thermal conductivity gradient. For many natural soils this conductivity gradient term turns out to be important. If omitted non-conductive processes would need to be invoked to explain the thermal data. To

assess the importance of the thermal conductivity gradient to the soil thermal regime, a representative period of early winter data (11/26-12/26/85) was analyzed. The least squared error between observed and modeled soil temperatures for this period using the formerly determined soil conductivity gradient (Chapter I, Thermal Conductivity) is 0.15°C for the 1.1 m deep reference volume. The same calculation using the mean thermal conductivity reveals a least squared error of 0.48°C , 220 % larger than optimal. Then, the least squared error was minimized, by finding the thermal conductivity constant over time and depth that produced the best fit between observed and modeled soil temperatures. This best fit mean thermal conductivity was $1.9 \text{ W m}^{-1} \text{ K}^{-1}$, which is 32 % smaller than the actual mean ($2.8 \text{ W m}^{-1} \text{ K}^{-1}$). Discrepancies are significant, and suggest that the thermal conductivity gradient can be omitted only in cases of completely homogeneous soils, despite its common absence in soil thermal analyses.

Frozen soils are known to contain unfrozen water at temperatures well below 0°C (Williams and Smith, 1989), which greatly increases the apparent heat capacity, requiring more energy to change the soil temperature and lowers the thermal conductivity near 0°C (McGaw et al., 1978). For soil from this study site, most of the water freezes above -1°C . From -1°C to -3°C the apparent soil heat capacity is augmented by only about 10 %, and below -3°C the contribution from unfrozen water is negligible (pers. comm. A. Tice, Cold Regions Research and Engineering Laboratory (CRREL)) (Figure 9). The unfrozen

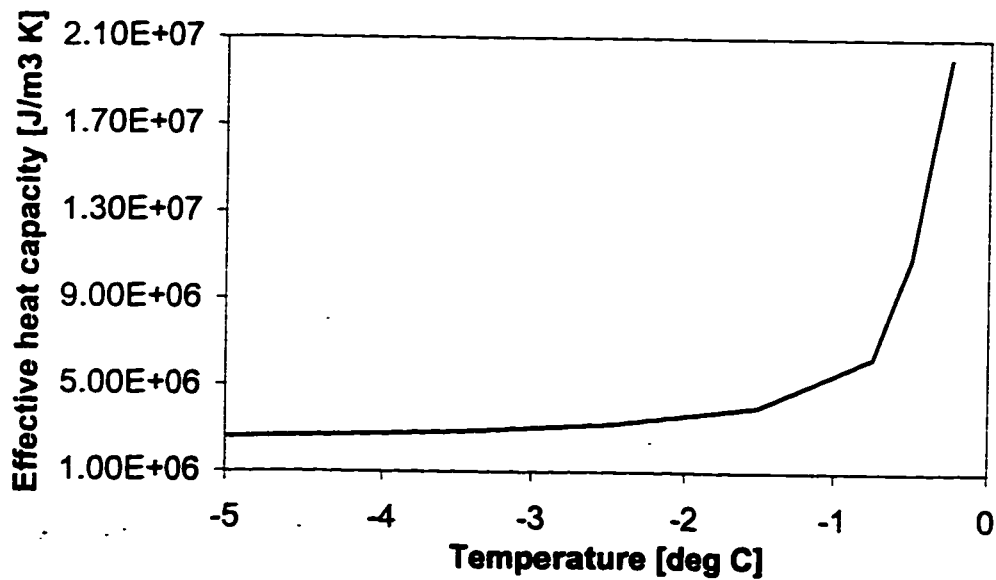


Figure 9: Effective heat capacity reflecting the influence of the unfrozen water freezing at temperatures below 0°C. For this soil, practically all of the water freezes above -3°C (based on NMR measurements of unfrozen water in samples from the site by A. Tice, CRREL) rendering the effect of unfrozen water at lower temperatures negligible.

water that freezes at temperatures below 0°C dictates the typical gradual departure (approach) of temperatures from (to) 0°C (Figure 10) characteristic to fine grained soils. Without this term, the modeled temperatures would depart abruptly from 0°C once all the water is frozen. The amount of unfrozen water content is soil specific, and omission of the term from models would lead to unrealistic results, particularly for fine-grained soils. Another well known phenomenon of freezing soils that is captured by the model is the formation of zero degree curtain, as the bulk of the soil water is freezing at a particular level, holding the soil temperatures at 0°C typically for many weeks.

The amount and location of ice growth and decay has considerable importance on soil thermal behavior. To model soil temperatures correctly over freeze up and melt periods, the temperature data were used to solve for rates of formation and melting of ice as a function of time and depth (see details below).

Taking into account all these factors, which are generally disregarded in soil thermal models, the modeling accounted for much of the observed thermal behavior and revealed reasonable values for thermal properties, closely resembling those measured in situ independently. There was generally no need to introduce non-conductive processes, except during the rapid warming events observed in the spring.

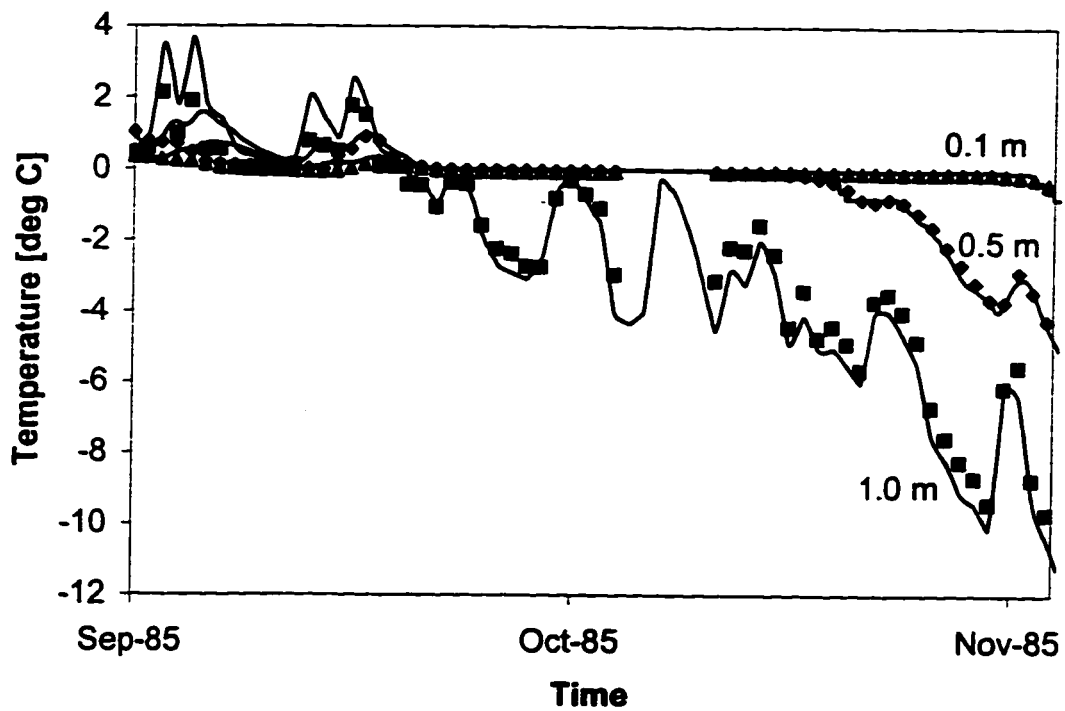


Figure 10: Modeled (lines) and observed (symbols) soil temperatures during the 1985 fall freeze up. Note the typical gradual departure of temperatures from 0°C, and the zero degree curtain that lasts over one month during the freeze up period due to the substantial amount of latent heat released as the bulk of the water freezes at 0°C.

CHARACTERISTIC SOIL THERMAL PHASES

I now summarize the primary characteristics of the soil thermal regime for thermally distinct periods of the year. The thermal field was modeled by making use of the observed soil surface temperature and heat flow, information on soil composition and thickness and on bedrock lithology, and assumed mean annual soil temperature 15 m below surface. The near surface soil thermal properties were solved by a one-dimensional standard heat transfer model (see chapter I). Modeled temperatures from 0.1 m to 1.1 m depth (0.1 m increment) are compared to observed temperatures.

During the summer conduction is the only significant heat transfer process. The propagation and attenuation with depth of the daily temperature signal is seen clearly in both modeled and observed soil temperatures (Figure 11). The vertical variation in soil thermal conductivity necessitates the inclusion of the dk/dz -term in the general one-dimensional diffusion equation (Figure 12).

Fall typically starts with persistently freezing air temperatures and light snowfall. The thermal regime is forced by sustained radiative energy loss at the ground surface resulting in slow conductive cooling in the soil. See Figure (10) for modeled and observed soil temperatures during fall freeze up. Considerable latent heat is released as water freezes, which establishes the widely recognized zero-degree curtain in the active layer. Soil thermal properties change progressively during this period as a result of extensive water

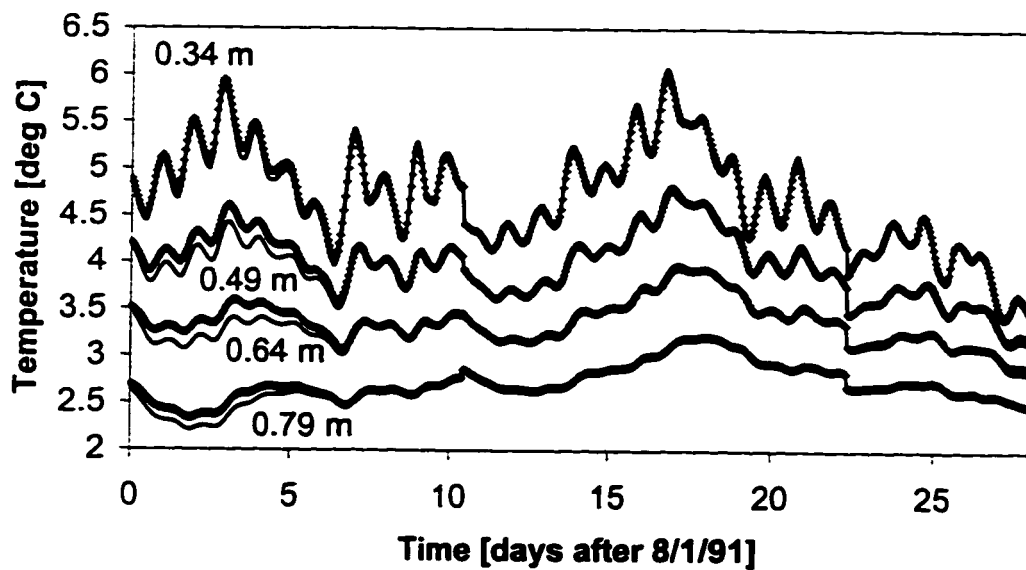


Figure 11: Excellent agreement between modeled (lines) and observed (symbols) soil temperatures during the 1991 summer, at four levels: 0.34 (warmest), 0.49, 0.64 and 0.79 m (coldest) below the surface.

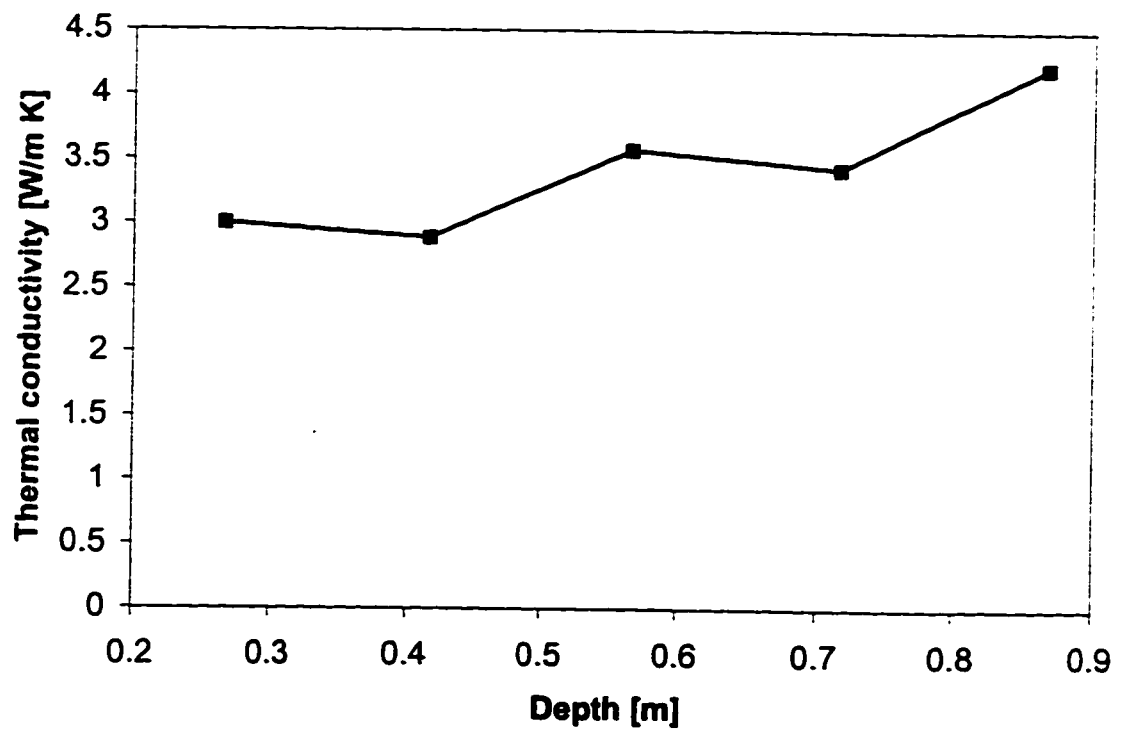


Figure 12: Summer soil thermal conductivity profile. The 0.2 m conductivity was measured in situ, for conductivities at lower depths see the Figure 8 caption for an explanation.

transfer and phase change that is manifested in considerable frost heaving. The soil moisture content and the amount of ice growth dictate the magnitude of latent heat effects. In the model, both the freezing of much of the water at 0°C and the progressive freezing of the remaining water at lower temperatures were taken into account through the latent heat term in equation (1).

The amount of ice that formed in the soil profile was determined by trial and error by allowing the ice amount in the model to evolve so that the correct timing of freeze up (temperature departure from 0°C) was reproduced at each level. Essentially all the heat is lost through the soil surface, hence the upper soil layers freeze first. Modeling the progressive descent of the freezing front, defined as the 0°C isotherm, makes it possible to calculate the amount of ice that forms as a function of time and depth. According to the model, the maximum ice concentration occurred 0.3 ± 0.05 m below the surface (Figure 13). No ice lensing took place near the surface, probably because the surface soil froze faster than it could draw water from below. This appears to contradict soil surface heave records from other years that show that considerable soil expansion occurs due ice growth within 0.2 m of the ground surface. This discord may arise from the summer before the observation period having been extremely dry. During July-September 1985, the precipitation was 33.2 mm which is the lowest in the record and less than 38 % of the average (for 1983-1991, existing data set). This suggests that the ground was drier than usual inhibiting the near surface ice growth.

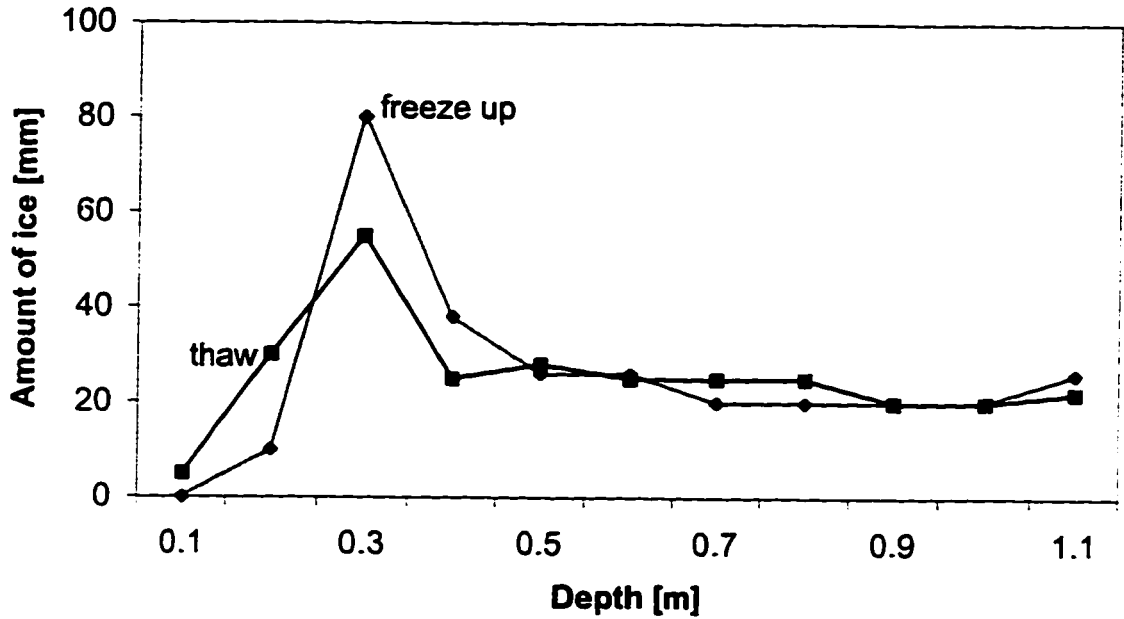


Figure 13: Modeled amount of ice in the soil per depth increment formed during the fall 1985 freeze up and melted during the subsequent thaw period. This was determined by allowing the ice amount in the model to evolve so that the correct timing of freeze up was reproduced at each level. The main modeled concentration of ice occurred 0.3 m below the ground surface. The total amount of ice thawed throughout the soil in the subsequent spring is within 2 % of the calculated amount formed in the fall, however the peak value at 0.3 m level is less pronounced during the spring presumably due to moisture redistribution during the snow cover period.

The total amount of ice that formed within the active layer was 296 mm of water equivalents, which is close to the suggested saturated water content for the same thickness. Moreover, the ice content profile obtained for the fall freeze-up is entirely consistent with the one deduced for the subsequent spring thaw (Figure 13), adding support for both. In conclusion, the model seems to capture the thermal behavior observed in the field, and hence the evolution of active layer soil temperatures during fall freeze up can be modeled by conduction with phase change.

Winter soil temperatures (Figure 14) are also generally dictated by conduction. During late spring (May-June), when considerable heat is provided by the sun to melt snow, the comparison of modeled and observed soil temperatures are suggestive of non-conductive events, probably moisture percolation into the frozen soil causing rapid warming as latent heat is released by freezing water. An independent heave record shows heave activity during same period (5/11 and 6/2/86), to lend further merit to this suggestion. During this period the 1.1 m thick soil layer warmed an average of 6°C, of which only 47 % appears to be due to conductive heating. In the model the soil temperatures were allowed to follow closely the observations. This required a non-conductive warming within the soil profile. Assuming that the warming is due to water percolating in the ground and freezing there, the amount of water that froze can be calculated. The heat liberated by the freezing of 35 mm of water could account for this warming.

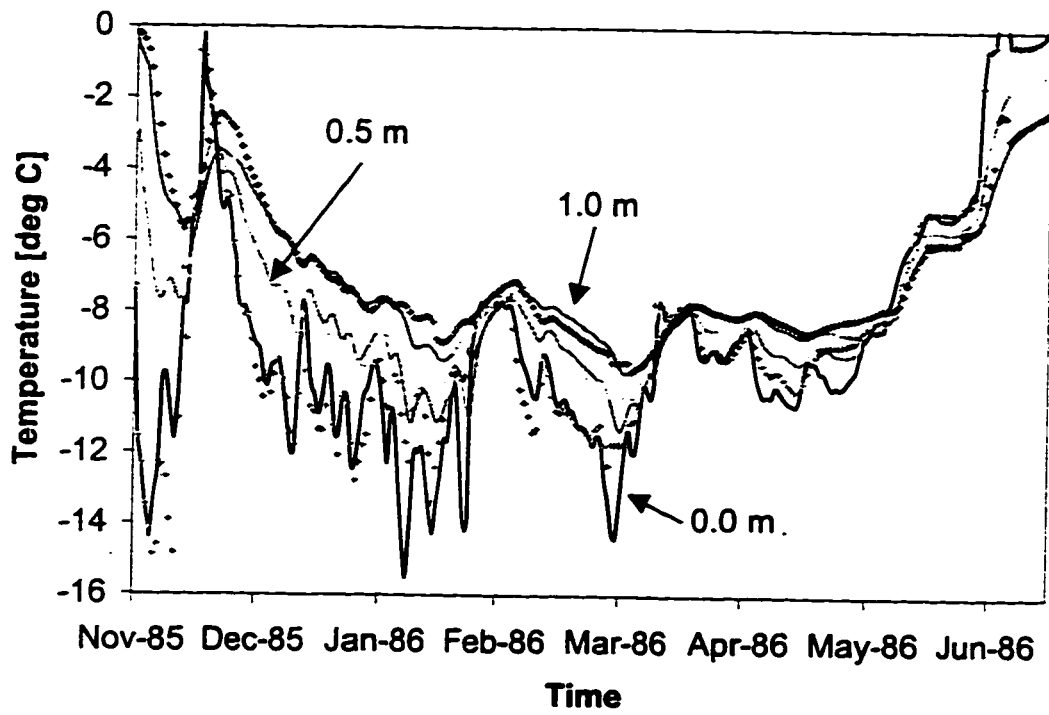


Figure 14: Modeled (lines) and observed (symbols) soil temperatures during the 1985/1986 winter.

To determine the amount of ice in the soil profile during spring melt; the ice concentration in the model was adjusted to reproduce the correct timing of the onset of thawing at each reference level. The amount of ice needed to satisfy the conductive model during the melt period was then compared to the amount of ice that was produced during the previous fall. The total amount of ice that formed during fall and the separately calculated amount that melted during the spring within the whole reference volume are within 2 % of each other. The ice content variation with depth is similar, but the peak value at 0.3 m level is less during spring melt (for ice content see Figure 13, and modeled and observed soil temperatures Figure 15). This can partly be explained by the percolation of water from thawed soil into the still frozen soil near 0°C, and the related advective transfer of heat, as shown by Mackay (1983).

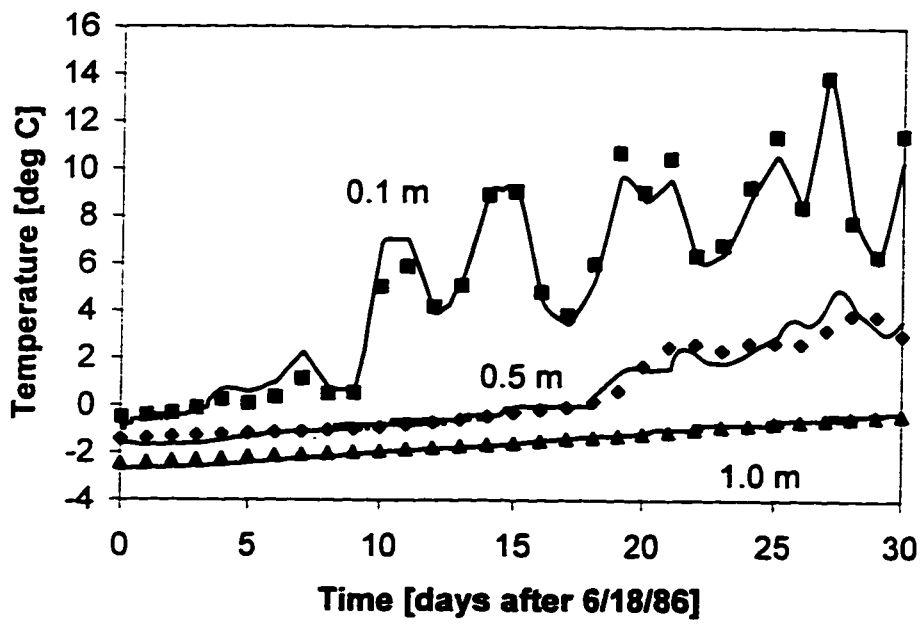


Figure 15. Modeled (lines) and observed (symbols) soil temperatures during the 1986 summer thaw.

CHAPTER III: ATMOSPHERIC FORCING

The soil thermal regime is driven by heat transfer processes, snow thermal properties and external atmospheric forcing including: net radiation, air temperature, and rain-on-snow events. Distinct forms of thermal forcing dominate during different seasons and are best described separately.

SUMMER

To define the length of the thaw season, the timing of snow disappearance was studied. The site was entirely snow free by 6/28 in 1991 and 1992, and in late August or early September the ground surface generally starts to cool and thereafter the soil gives off heat. Thus the length of the thaw season is taken to be the two months period 7/1-8/31. The average air temperature and average net radiation at the field site between 7/1-8/31/91 are 3.5°C and 70 W m⁻².

NET RADIATION AND AIR TEMPERATURE

After the 1.5 m thick active layer has thawed, the near surface (0.2 m) soil heat flow (G) is primarily a function of net radiation and air temperature (Figure 16).

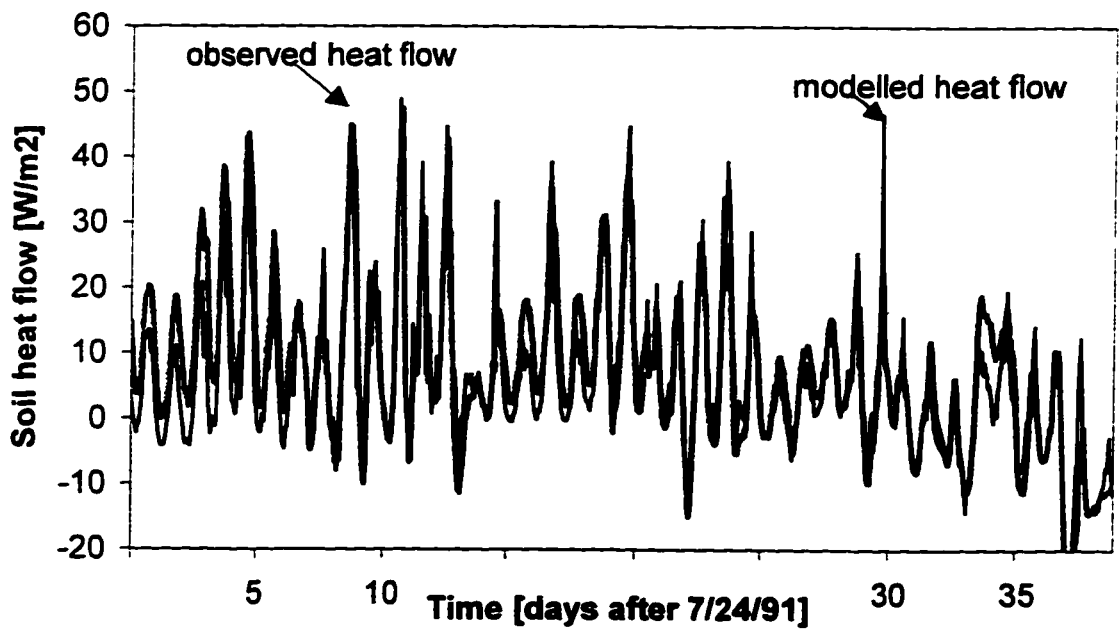


Figure 16: Soil heat flow 0.2 m below surface during summer 1991: measured and modeled, based on net radiation and air temperature. Positive values indicate heat flow into the soil.

The least squared difference between observed and modeled soil heat flow (W m^{-2})(7/24-8/31/92) was used to optimize the linear regression:

$$G = \alpha R_{\text{net}} + \beta T_{\text{air}} - \gamma, \quad r^2 = 0.9 \quad (5)$$

Where α is 0.121 [dimensionless], β is 2.38 [$\text{W m}^{-2} \text{ }^\circ\text{C}^{-1}$], γ is 8.83 [W m^{-2}], R_{net} is the observed net radiation at the site [W m^{-2}] and T_{air} is the observed air temperature 1 m above the soil surface at the study site [$^\circ\text{C}$].

When comparing soil heat flow at 0.2 m depth to net radiation and air temperature, the time lag for the thermal signal to propagate from the surface to that depth must be taken into account. In this case, the best correspondence was found for a two hour delay, which is consistent with the expected lag between instantaneous changes at the surface and the response at 0.2 m for soil with a representative thermal diffusivity ($10^{-6} \text{ m}^2 \text{ s}^{-1}$).

The ratio of soil heat flow to net radiation was 0.18 for the period 7/24-8/31/91. This parameter has been assessed in other studies as well. For example, in diverse tundra areas near Hudson Bay and at Axel Heiberg Island, Canada; Kanqerlussuaq, Greenland; SW Alberta, Canada and Niwot Ridge, Colorado, the ratio varies from 0.036 to 0.18 and averages 0.12 (Rott and Obleitner, 1992; Bowens and Bailey, 1989; Weick and Rouse, 1991; Rouse, 1987; Rouse, 1984; Rouse et al., 1987; Isard and Belding, 1989; Ohmura,

1982). The Spitsbergen value is relatively high, probably because all other study sites were at least partially covered with organic material, which provide considerable thermal insulation to the surface.

WINTER

During much of the cold season the field site is covered with snow that acts as a very effective insulator. In Spitsbergen, soil is generally thoroughly frozen before a thick (>1 m) snow cover becomes established, usually in late November or December.

Several processes and characteristics of the snow cover affect the soil thermal regime: surface temperature, snow thickness and density, constructive and destructive snow metamorphism, heat conduction and advection, and latent heat effects. These are considered below.

AIR TEMPERATURE, SKY TEMPERATURE AND SNOW SURFACE TEMPERATURE

Air temperature is traditionally used as a boundary condition or as a surrogate for snow surface temperature. I will show that there is a considerable difference between these temperatures, and furthermore that snow surface temperature can be correlated with the sky temperature, allowing a direct link between Global Circulation Models and soil thermal models.

In Ny Alesund, both air temperature (minimum and maximum air temperatures twice a day for preceding interval, GMT 06:00 and GMT 18:00) (pers. comm. Inger Hanssen-Bauer; Norwegian Meteorological Institute) and the upward component of long wave radiation (Hisdal, Finnekasa and Vinje, 1992) were recorded intermittently during the study period (periods of data coverage during 1986: 1/1-1/27, 2/14-28, 3/1-14,16,4/2-27,29-30). The study site and the whole peninsula including the Ny Alesund research station were completely snow covered during these periods.

Long wave radiation measurements (daily averages of hourly measurements) can be used to calculate the snow surface temperature using the Stefan-Boltzmann law.

$$E = \varepsilon \sigma T_{\text{surface}}^4 \quad (6)$$

where E is radiative energy [W m^{-2}], ε the gray body emissivity (for snow ε is 0.985-0.990 (Dozier and Warren, 1982)), σ the Stefan-Boltzmann constant ($5.67 \cdot 10^{-8} \text{ W m}^{-2} \text{ K}^{-1}$), and T_{surface} the absolute surface temperature [$^{\circ}\text{K}$].

Snow surface temperature T_{surface} [$^{\circ}\text{C}$], is strongly correlated with air temperature, T_{air} [$^{\circ}\text{C}$] measured 2 m above the soil surface, for all periods when data were available.

$$T_{\text{surface}} = 0.88 T_{\text{air}} - 3.74, \quad r^2 = 0.91 \quad (7)$$

However, based on daily averages, the snow surface temperature is up to 3.7°C lower than the standard air temperature during the same time period. Similarly, Weller and Holmgren (1974) showed a typical winter temperature difference between the snow surface and the air in Alaska (2 m height) of 3.8°C (figure 6 in: Weller and Holmgren, 1974). This arises because heat is primarily lost by radiation to the sky from the snow surface, rendering it colder than the air. Equation (7) is used in this work to transfer air temperatures into snow surface temperatures in Ny Alesund. The relationship between temperatures at the tip of the peninsula, where the study site is located, and Ny Alesund, which is ~10 km further inland, is considered in the next section.

To link General Circulation Models to soil temperature models, the snow surface temperatures can be empirically correlated with sky temperatures (downward long wave radiation) to permit a direct link to Global Climate Models that generally track moisture and temperature evolution at several levels in the atmosphere (Hartmann, 1994). Atmospheric moisture and corresponding air temperature can then be used as input for atmospheric radiative models to determine the effective downward radiation from the atmosphere, and hence the snow surface temperature.

In Ny Alesund, the downward long wave radiation component was also measured (Hisdal, Finnekasa and Vinje, 1992). By assuming, the sky to be a perfect emitter, one can calculate a corresponding sky temperature (Equation 6) that effectively integrates

over the height of the boundary layer (generally from the surface to up to 1 km) and over all emitting particles (among the most important being water vapor and carbon dioxide).

During the study period (1/1-3/31/86) the snow surface temperature, T_{surface} , and downward radiative sky temperature, T_{sky} , were well correlated.

$$T_{\text{surface}} = 0.65 T_{\text{sky}} - 2.34 \quad r^2 = 0.91 \quad (8)$$

where both temperatures are expressed as °C.

AIR TEMPERATURE DIFFERENCE BETWEEN FJORD INTERIOR AND MOUTH

For the main 1985/86 study period, the air temperature was not measured at the field site but it can be estimated from meteorological records in Ny Alesund. Whereas the field site is on the tip of the Broegger peninsula, about 2 km from the open ocean, the research station in Ny Alesund (where the meteorological data are measured) is located in a fjord about 10 km from the open ocean. In the winter in western Spitsbergen, the air in the fjord interiors tends to be 2 to 5°C colder than at fjord mouths (Hanssen-Bauer, Kristensen Solas and Steffensen, 1990). The reverse temperature difference (fjord interior warmer than fjord mouth), which increases with distance from open ocean due to the increased continentality, occurs during the summer (Schmitt, 1993). For example the

mean air temperature at the field site for July-August, 1991 was 1.3°C lower than in Ny Alesund.

To assess this snow surface temperature difference between Ny Alesund and the field site during the 1985-86 study period, a 62 day period of no precipitation was chosen (starting 11/23/85). Snow depth was assumed to be constant during this period for two reasons. First, changes in snow thickness due to drifting are assumed to be minimal, because directly prior to this period there was a pronounced warming due to a major incursion of Atlantic air that would have sintered and stabilized the snow surface, inhibiting further mobilization of snow. Second, sublimation is not an effective snow removal process in the dark winter in this relatively warm and moist environment, where average relative humidity, during even the coldest months is above 70 %.

I now proceed to estimate the probable combination of constant snow depth and offset in snow surface temperature between Ny Alesund and the field site during the 62 day period of the 1985-86 study year. I use snow depth and snow surface temperature as inputs for a one dimensional thermal conduction model to find the least squared difference between observed and modeled soil surface temperatures at the field site. The “best” combination is a snow depth of 0.1 m and for the field site snow surface to be 1.5°C warmer than at Ny Alesund (Figure 17). By making use of the air temperature offset, I can compute the

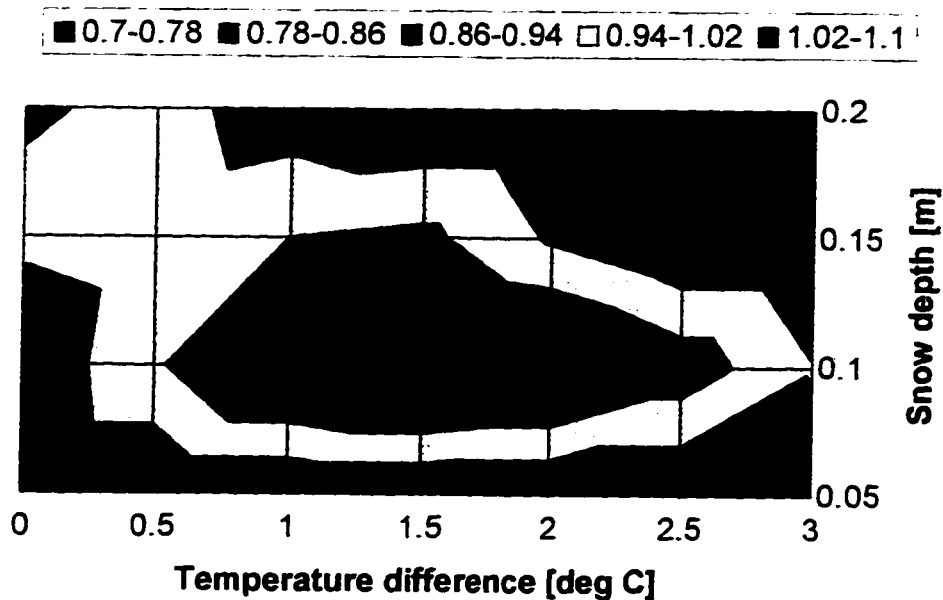


Figure 17: RMS-difference between modeled and observed soil surface temperatures as a function of two unknowns: snow depth at the field site and of the difference between the snow surface temperature at the fjord mouth and in Ny Alesund. This was determined by a one dimensional thermal conduction model by allowing these unknown parameters to vary. The RMS-minimum suggest a unique combination: a snow depth of 0.1 m and the snow surface being 1.5°C warmer at the field site than in Ny Alesund.

air temperatures for the field site for the period when direct measurements are not available. This in turn is used in the soil temperature model to calculate the snow surface temperature.

SNOW HEAT TRANSFER

The soil at the study site tends to be solidly frozen before the snow cover is established. Subsequently soil surface temperatures depend only on snow depth, thermal properties both above and below soil surface, and heat transfer processes in snow.

Two main heat transfer processes in the snow pack are generally recognized: conduction and heat advection due to air and vapor motion. Advection was documented in Alaska (Sturm and Johnson, 1991) where conditions for this were particularly favorable: shallow snow thickness (0.6 m), warm soil surface (soil was generally not frozen prior to the snow cover becoming established), cold snow surface, and porous snow pack. Air convection cells in the snow in Alaska developed largely because of spatial differences in soil surface temperatures, which were primarily caused by the different amounts of moisture in the freezing soils (Sturm and Johnson, 1991).

In Spitsbergen air convection in the snow pack appears quite unlikely. The mid-winter snow depth at the study site generally exceeds a meter, about twice that for the Alaska sites studied by Sturm and Johnson (1991). Therefore, snow densification proceeds further in Spitsbergen thereby reducing the snow porosity. For most of the winter,

temperature gradients that drive the free convection in the snow pack in Alaska, were larger than in Spitsbergen by an order of magnitude or more. Furthermore air convection has never been documented in thick, dense snow pack and it is unusual in most natural snow covers (Sturm et al., 1996). Essentially, all heat transfer in snow at the study site is therefore likely to be by conduction.

All thermal properties of snow depend on density. Sturm et al. (1996) have recently proposed that for snow, with densities (ρ_{snow}) between 156 and 600 kg m⁻³, the thermal conductivity, k_{snow} [W m⁻² K⁻¹], is:

$$k_{\text{snow}} = 0.138 - 1.01 \cdot 10^{-3} \rho_{\text{snow}} + 3.233 \cdot 10^{-6} \rho_{\text{snow}}^2 \quad (9)$$

It is recognized (Sturm et al. 1996), that the thermal conductivity of snow depends also on ambient temperature, but more data are needed before reliable conclusions can be drawn. The heat capacity of snow is proportional to its density as well: ($\rho_{\text{snow}} C_{\text{ice}}$), (C_{ice}) being 2100 J kg⁻¹K⁻¹.

INITIAL DENSITY OF SNOW

The density of freshly falling snow depends on air temperature and wind speed at the time of precipitation. Observed fresh snow densities during cold (-10°C), calm conditions range from 60 kg m⁻³ to 100 kg m⁻³ and near 0°C, 100-200 kg m⁻³ (Dunne and Leopold,

1978; Seligman, 1980). Winter air temperatures in Spitsbergen are only moderately low, averaging -11.3°C from November to May, and major precipitation events are often associated with near 0°C air temperatures. Hence, snow in Spitsbergen is expected to be relatively dense.

Snow density can also be influenced by winds as they tend to fragment and redeposit snow crystals, resulting in denser packing. Under calm conditions, Mellor (1964) reports snow density of 100 kg m^{-3} , whereas with strong winds, densities can reach 300 kg m^{-3} . Average wind speeds during winter months are from $1\text{--}9\text{ m s}^{-1}$, and winds exceeding 17 m s^{-1} occur less than once a year. As the field site is relatively warm and moderately windy, the initial density of freshly fallen snow is assumed to be 150 kg m^{-3} . It is shown below that this is not, however, a very critical assumption. This estimate is well within the range of values found in an existing two year long data set of snow density from Hornsund (200 km south of the field area), which shows initial snow densities around 200 kg m^{-3} (Mietus, 1991).

SNOW METAMORPHISM

Snow thermal conductivity is a function of post-depositional metamorphic changes in snow density and structure (Sturm et al., 1996). Snow metamorphism can be divided into two phases: a rapid early stage that proceeds relatively fast at a constant rate until snow reaches a density of 250 kg m^{-3} , and slow late stage that depends on the weight of overlying snow mass.

Destructive metamorphism (early stage) sets in once snow settles on the ground (Gunn, 1965), as snow crystals tend to minimize their surface free energy. Density can increase by 1 % hr⁻¹ until densities reach 150 kg m⁻³, and then can reach relatively stable value of 250 kg m⁻³ in two (near 0°C) to three days (at -11°C) (Jordan, 1991). Therefore, the considerable uncertainty of the initial snow density is not important for the overall modeling of the soil thermal regime because it affects only the very few first days after each snowstorm.

The densification process (late stage) continues slowly, due to the weight of overlying snow mass, as shown by Kojima (1967). The following quantitative representation (Equation 10) is generally accepted (e.g. Mellor, 1964; Yen, 1981; Grey et al., 1995; Yamazaki et al., 1993; Goodrich, 1982), and was used in this study to model snow densification after the initial destructive metamorphism.

$$\frac{1}{\rho_s} \frac{\partial \rho_s}{\partial t} = C_1 W_s \exp(-C_2 \rho_s) \exp[-0.08(T_0 - T)] \quad (10)$$

where: ρ_s is the snow density [Mg m⁻³], t the time [hr], C_1 and C_2 Kojima's constants, respectively = 4.75 m⁻¹ hr⁻¹ and 21 m³ Mg⁻¹, W_s the weight of snow pack, in water equivalent [m], $T_0 = 273$ °K, T is the snow temperature [°K].

The formation of depth hoar, flaky ice crystals at the bottom of the snow pack, can complicate the thermal analysis of the snow/soil system significantly (Zhang and Osterkamp, 1993; Zhang et al., 1996). It has been shown, however, that depth hoar grows only if the thermal gradient in the snow generally exceeds $25^{\circ}\text{C m}^{-1}$ (Marbouty, 1980., Colbeck, 1983., and Akitaya, 1974 as shown in Sturm et al., 1995). Based on the modeled snow surface temperature, snow depth and the observed soil surface temperature, the average snow thermal gradient in the 1985/86 winter at the Spitsbergen study site was $4.3^{\circ}\text{C m}^{-1}$. Only during 10 % of the period of total snow cover did the gradient exceed $25^{\circ}\text{C m}^{-1}$. Based on a model of depth hoar growth rate (Marbouty, 1980; Brun, 1992), the depth hoar crystals would grow less than 0.2 mm in diameter, even if all the necessary conditions described above were met in one continuous event. For comparison, fully developed depth hoar flakes are found to be >10 mm in diameter in Alaska (Trabant and Benson, 1972). Therefore, depth hoar is most likely to be insignificant in altering the thermal conductivity structure of the snow in this field area. In addition, the occasional rain on snow (see details in next section) would destroy the possible depth hoar, had it formed.

SNOW DEPTH

Snow depth is one of the parameters defining the heat transfer between the permafrost and the atmosphere, but it had to be inferred for this remote field site where direct observations were largely unavailable during the 1985-86 study period. I used the general

thermal diffusion equation with known or derived snow surface temperature, soil surface temperature, snow density and thermal properties, and monitored snow accumulation in Ny Alesund (preceding 24 hours at GMT 06:00), to establish the snow depth history that was most consistent with the observed soil surface temperatures. It is assumed that the progressive accumulation of snow with time at the field site is generally similar to that in Ny Alesund.

Manual measurements at the field site during four separate winters, show typical snow depths of 1.0 to 1.2 m through most of the winter and spring (Figure 18). Snow depth was also studied by measuring the vertical profile of temperatures in and above the snow, based on the concept that whereas steep thermal gradients are expected in the snow due to its low thermal conductivity, the air directly above the snow surface ought to be essentially isothermal (see section on: Air Temperature, Sky Temperature and Snow Surface Temperature). This technique has the virtues of being rugged, economic, and free of riming problems, that plague the commonly used sonic ranger, and it also provides direct data on the snow thermal regime. Problems with the method are the wind scour around the PVC pipe holding the thermistors, and of preferential heating and melting of

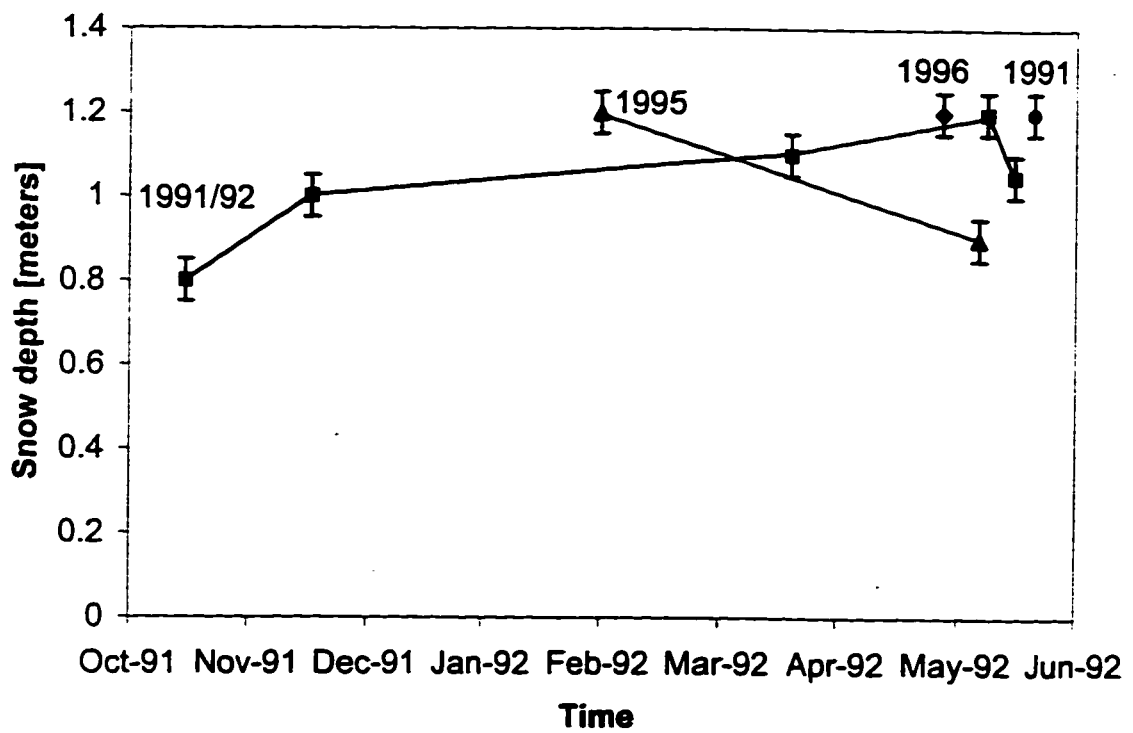


Figure 18: In situ manual snow depth observations at the field site during four winters, showing snow depths do not vary much from year to year and tend to be slightly more than 1 m through most of the winter.

snow during the Spring due to long wave radiation emitted by the pipe as warmed by the sun. Both of these complications tend to result in underestimates of the actual snow depth by perhaps as much as 0.2 m.

When this device was used initially, the depth/temperature record was tested against three manual measurements at the site, spanning one year. The snow temperature records revealed a record consistent with the observations, but the resolution of the snow depth was poor because of the large spacing between the upper thermistors (located at 0.9 and 1.6 m above soil surface). This procedure has been refined and is currently being field tested by comparing the snow temperatures against simultaneous recordings from a sonic snow depth sensor.

RAIN ON SNOW

Using the snow surface temperatures as derived above, there were several distinct periods of rapid warming during which heat conduction through snow could not account for the observed soil surface temperature. Hence, either the snow surface temperature or the conduction assumption, or both, are invalid during these periods. As different scenarios were tested, it was found that:

- 1) The observed abrupt warming at the soil surface cannot be reproduced by employing the maximum possible snow surface temperature (0°C), and hence exceptionally high snow surface temperatures cannot fully explain the discrepancy.

2) The assumed dominance of heat conduction is likely to have broken down during the warming events, as considerable latent heat may have been transferred to the base of the snow by water percolation and refreezing.

3) Snow could have been eroded away, thinning the cover considerably. This is unlikely, because the site is situated in a swale that favors deposition rather than scouring. In addition, the high frequency temperature variations, characteristic of a thin snow cover, are not seen in the soil surface temperature record. Moreover, as explained below, these warming events were times of heavy precipitation and thickening snow cover.

Detailed inspection of weather records confirmed that these warming events were characterized by heavy precipitation consisting of rain as well as snow in Ny Alesund, and most probably at the nearby field site. Taking the 3/15/86 event, for example, the observed soil surface temperature increase can be attained if the snow/soil interface (a 0.1 m-thick model increment comprised of both snow and soil) is warmed by the latent heat released by about 4.8 mm of water freezing at the soil surface using a representative heat capacity for the snow-soil combination. During this three-day period (3/14-16/1986), 30 mm of slushlike precipitation (mixed water and snow) were recorded by the Ny Alesund weather station. Further proof of water percolation and refreezing is a mid winter (1/30/94) in situ observation of a thick ice layer below the snow cover at the soil surface at the field site (pers. comm. G. Aasebostol 3/8/94). Similar ice layers at the soil surface

below snow pack in the High Arctic are widely recognized (Woo and Heron, 1981; Marsh and Woo, 1984a, Marsh and Woo, 1984b; Woo, Heron and Marsh, 1981), and suggest water percolation and refreezing are widespread.

Ny Alesund meteorological records reveal that for the 1983-1990 period (existing data set) each winter was punctuated by several slushlike precipitation events. The 1985-1986 winter was one of the driest in terms of the number of such events that occurred. Moreover, no major rainfall (rain > 5 mm/event) took place, as was the case in 50 % of the winters. In terms of amount of slush and water together, the winter was average. However, it has to be kept in mind that errors of up to 30-50 % are related to measurements of winter precipitation, due to wind effects (Goodison, et al., 1981, p. 204-207).

The experimental snow temperature profile through the 1995/96 winter, revealed three major rain-on-snow events. After the second event, the soil surface remained at or near the freezing point for a considerable period (Figure 19). The 1995/96 mid-winter (1/1-3/31/96) near-surface soil temperatures were more than 9°C warmer than in 1985/86 (Figure 14), whereas the air temperature was only 3°C warmer. This clearly shows the major effect of rain-on-snow on soil temperatures. The record of heat flow, 0.05 m below soil surface at the field site (1/1-3/31/96), also contradicts the general view of Arctic soil thermal behavior during the snow cover period, because the soil was receiving thermal energy from the snow instead of losing it, for 64 % of the reference period (Figure 20).

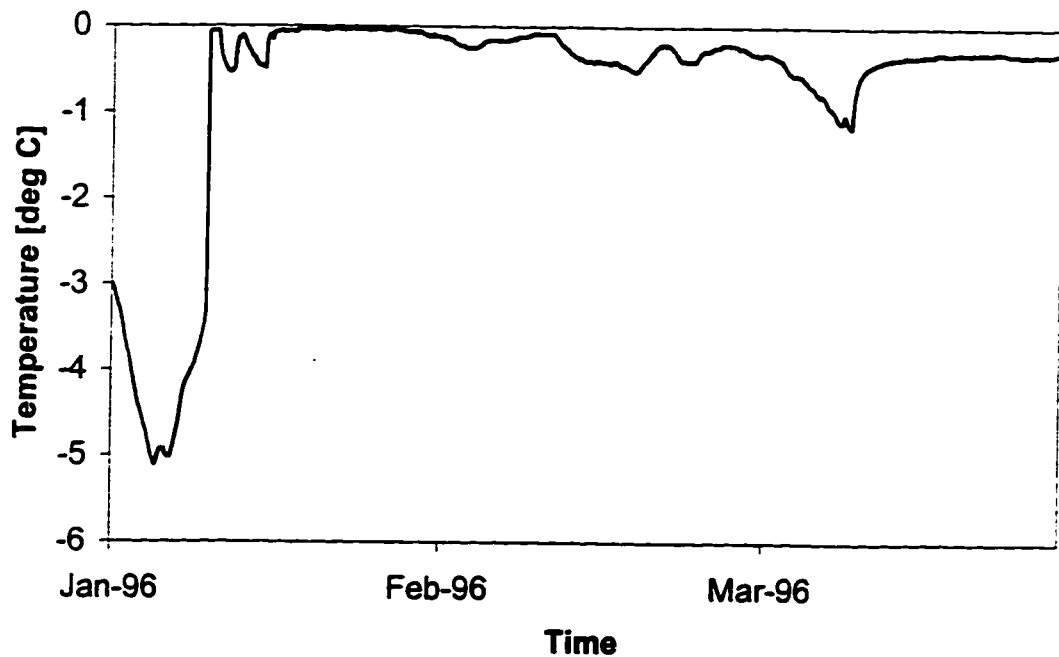


Figure 19: The soil surface temperature through the 1995/96 winter, revealed three very large rain-on-snow events. After the second event (1/10/96), the soil surface remained at or near the freezing point for nearly 3 months, which is about 9°C warmer than the reference winter in 1985/86. Only about one third of this warming is due to higher winter air temperature in 1995/96, indicating that the bulk of the soil warming is due to increased rain-on-snow activity.

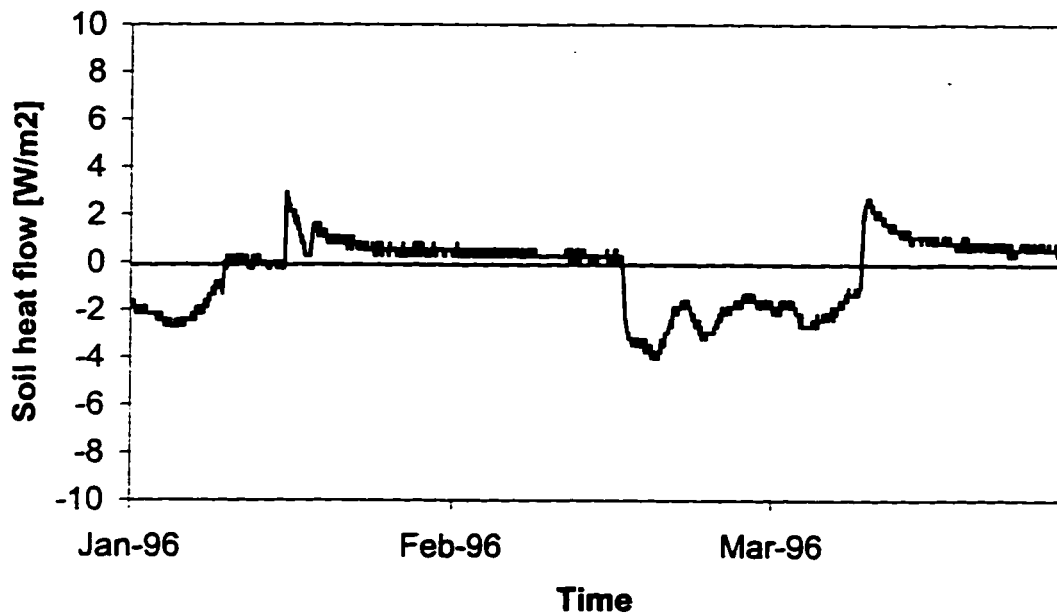


Figure 20: Soil heat flow 0.05 m below the surface during the 1995/96 snow cover season. Positive values indicate heat flow from the snow /soil boundary to the soil. This record conflicts the general view of Arctic soil thermal behavior during the snow cover period, since the soil was receiving thermal energy from the snow instead of losing it, for 64 % of the reference time. This differs significantly from a corresponding 18 % in winter 1985/86, and 2 % in winter 1994/95 (based on an incomplete record).

This differs significantly from the corresponding 18 % for the 1985/86 winter, and 2 % for the 1994/95 winter (based on an incomplete record).

CHAPTER IV: SENSITIVITY OF SOIL HEAT FLOW TO CURRENT ATMOSPHERIC VARIABILITY

In order to better anticipate the response of the soil thermal regime to changing climatic conditions, I examine quantitatively: 1) the magnitude of the natural variability (one standard deviation from average) of each primary atmospheric and environmental factor that dictates soil temperatures, and 2) the sensitivity of the soil thermal regime to these primary factors, by making use of the model developed in chapters I-III.

The winter 1985/86 and summer 1991 and 1992 are used as reference periods. The model is run with one external variable perturbed at a time; the influence of other variables is examined sequentially. To compare the relative importance of different atmospheric factors and time periods of varying length (seasons), the absolute deviations in energy flow are integrated over the season and then normalized over one year, to yield comparable values in $W m^{-2}$. These perturbations in soil heat flow are important as is evident from comparison with estimated changes in heat flow from permafrost (Lachenbruch et al., 1982). Based on detailed analysis of temperature profiles in boreholes hundreds of meters deep, they concluded that the warming seen in permafrost temperatures in Alaska results from a net accumulation of heat in the earth at a rate of 0.1 to 0.2 $W m^{-2}$ for decades to a century.

The sensitivity of the soil thermal regime to four primary types of external forcing were examined: 1) seasonal air temperature, 2) rain-on-snow events (rain falls on snow and subsequently percolates through the snow pack), 3) snow depth; and 4) net radiation.

1. Air temperature is the most often used forcing in studies of the sensitivity of soil temperatures to climate change, probably because of its widespread availability. Herein, I consider changes in air temperature for each season and their respective effect on soil heat flow. From year to year, the mean seasonal temperature varies significantly. Standard deviations of air temperatures over each season in Ny Alesund for the 1975-1989 period are: 1.0°C from September to October, 2.0°C from November to April and 0.34°C from June to August. Below, I use these standard deviations as an index of the magnitude of likely changes in surface temperature for the field site, and calculate how much these would change soil heat flow for each season.

a) Autumn. The mean reference heat flow out of the soil during this period is 15.1 W m⁻². Perturbing the mean Autumn air temperature by one standard deviation (1.0°C) changes the mean seasonal and annual soil heat flow by ± 2.4 and 0.40 W m⁻², respectively.

b) Winter. For the reference case (winter 1985/86), the mean heat loss from the soil (November-April) is 5.6 W m^{-2} . Altering air temperature by 2°C over the same period causes a mean deviation of $\pm 1.5 \text{ W m}^{-2}$. The mean annualized difference to the reference case is $\pm 0.75 \text{ W m}^{-2}$ (Figure 21).

c) Summer. Air temperature changes during the summer are generally small because air masses do not differ substantially in temperature and moisture during this period. The relation between air temperature and soil heat flow (see chapter III) is used to determine the effect of changing summer air temperature on soil heat flow. The natural variability of summer air temperature (Jul-Aug) is 0.34°C . The corresponding change in soil heat flow for the season is 0.78 W m^{-2} , which amounts to a change averaged over a year of 0.13 W m^{-2} .

2. Rain on snow. The Spitsbergen winter is commonly interrupted by storms blowing in from the North Atlantic and causing rapid warming of the air, often accompanied by rain on snow. At least in some cases, rain and snow melt percolate through the snow pack to the soil/snow interface and freeze there, delivering a considerable amount of energy. Here I proceed to quantify the effect of this phenomenon on soil heat flow. During the winter of the 1985/86 reference year, an estimated 4.8 mm of water froze at or near the soil surface (Chapter III). The released latent heat that was delivered below the thick snow cover, corresponded to a mean annual effective heat flow

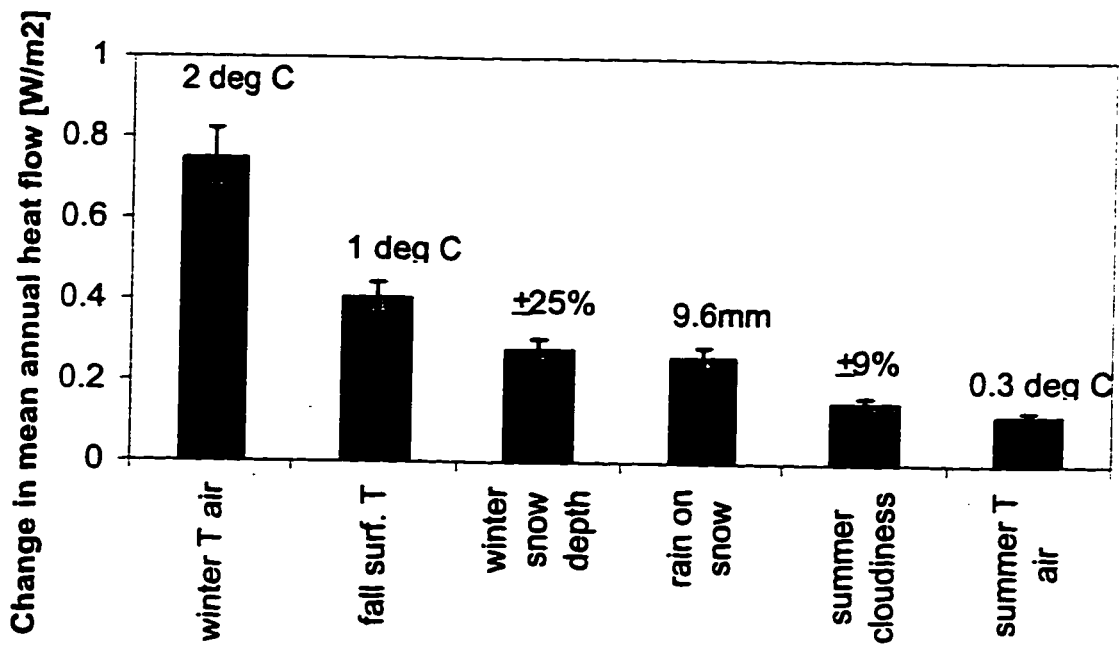


Figure 21: Sensitivity of mean annual soil heat flow to variation in surface forcing, and $\pm 10\%$ sensitivity test. Mean annual soil heat flow is affected most by variations in winter air temperature. Contrary to intuition, changes in summer cloudiness or air temperature are less important.

contribution of 0.14 W m^{-2} . Since the actual amount of rain that fell during a winter is not known (the research station reports only the total amount of precipitation; snow and water are not differentiated), I counted all events for which the research station reported either rain or slush in a winter, and found that the winter 1985/86 was one of the driest on record, with only three events. In other years the number of such events ranged from 2 to 9. The total amount of rain and slushlike precipitation (January-March) was 30 mm, which is only about half of the average (58 mm). Assuming that the amount of water reaching the base of snow pack scales with the total amount of rain and slush in a winter, the mean and the standard deviation of the winter rain that froze at the base of the snow pack can be estimated, based on the available record of winter rain and slush. The average amount of rain is 9.6 mm, and standard deviation is also 9.6 mm. This corresponds to a 0.56 W m^{-2} seasonal and a 0.28 W m^{-2} annual change in soil heat flow (Figure 21).

3. Snow depth. Ny Alesund meteorological records (Hanssen-Bauer et al., 1990) show that the mean winter (September-May) precipitation is 293 mm water equivalent (1975-1989). The standard deviation of the cumulative snow depth at the end of May is 26 %. On a nearby glacier (Broeggerbreen, 7 km SW from the field site) the standard deviation of water equivalent winter accumulation over the 1967-1991 period is 22 % (Hagen et al., 1993); for the adjacent Lowenbreen it is 25 % (Hagen and Liestol, 1990). The standard deviations of the annual snow accumulation from

five other glaciers in Spitsbergen within 150 km of the field site ranges from 11 to 20 % (Hagen and Liestol, 1990).

Monthly mean snow depth measurements are available also from Svea Gruva 1981-1993 (150 km South of the research site)(pers. comm. I. Hanssen-Bauer, 1995). The standard deviation of total annual snow depth, which should be comparable to the glacier accumulation data, is 24 % there. To establish how the timing of the accumulation differs from year to year, which also affects the net soil heat flow, I calculated average monthly snow depths. The standard deviation of monthly snow depth averaged 27 %, suggesting that snow cover builds up with time in a similar manner each year.

Summarizing the data from different localities and sources in Spitsbergen, gives similar results, namely that year to year standard deviation in snow depth is approximately 25 % or less. This is consistent with occasional point measurements at the field site on four different winters, which all revealed a very similar snow pack (Figure 18).

To study the modeled response in soil heat flow to changing snow depth, a ± 25 % change in snow depth relative to the 1985-1986 winter was invoked throughout the winter, using the same evolution in snow depth with time as that inferred for the reference winter. The mean changes in seasonal soil heat flow were -0.56 W m^{-2}

which amount to $+0.46 \text{ W m}^{-2}$ and annualized differences of -0.28 W m^{-2} and $+0.23 \text{ W m}^{-2}$.

4. Solar radiation is the most important energy source to heat soil in the summer. Net radiation, comprised both short and long wave radiation, contains direct and diffuse contributions from the sun as well as contributions from clouds and aerosols. Increased cloudiness reduces solar radiation and increases downward long wave radiation at the surface, because of the greater cloud optical thickness and increased moisture in the boundary layer. However, the clear sky short wave contribution is larger than the long wave part from clouds during overcast, and therefore increased cloudiness results in an overall cooling and decreased soil heat flow. Generally, 50-60 % of days are overcast in Ny Alesund in the June-August period (Hanssen-Bauer et al., 1990), the rest being either partly cloudy (majority) or clear.

To study the natural variability in net radiation, existing data from the Ny Alesund research station during the 1982-1987 period were examined (Hisdal et al., 1992). The mean net radiation for July and August is 88 W m^{-2} . Its standard deviation is 7.5 W m^{-2} , which corresponds to a mean natural variability of $\pm 8.6 \%$. Since the sun is the primary source of radiative energy, similar calculations were performed for the downward short wave component only (direct and diffuse). The calculated differences in down-going short wave radiation were even smaller than those for the net radiation. The relation between net radiation, air temperature and soil heat flow

(Chapter III, equation (5)) enables me to evaluate the effect of this variability on soil heat flow. The increase in summer soil heat flux due to an 8.6 % increase in net radiation amounts to a seasonal and an annualized increase in heat flux of 0.96 W m^{-2} and 0.16 W m^{-2} , respectively.

The overall effect of fog is implicitly included in changes in radiation treated in the previous paragraph, but because fog blocks short wave radiation so effectively, it merits separate discussion. Fog causes the largest deviation in radiation from its mean values on a daily basis, but as fog occurs very seldom, the overall effect is not significant. According to fog records (1975-1989), mean monthly frequencies of fog were 1.6 % in July and 2.5 % in August (Hanssen-Bauer et al. 1990). A substantial increase in the frequency or persistence of fog would have a profound effect on summer soil temperatures, but the annual natural year to year variability in the frequency of fog for summer is only 4.5 % (Alfred Wegener Institute, Koldeway Station, Ny Alesund, weather records, July-August, 1991-1996).

According to the model study of the sensitivity of the soil energy budget model to natural variations in atmospheric forcings, changes in winter air temperature have the greatest potential to change soil heat flow at the study site. Hence, year to year changes in mean permafrost temperatures are most likely to be caused by changes in winter air temperature. Contrary to intuition and widely held views, current changes in summer cloudiness or air temperature have only a minor effect on the overall soil

energy balance (Figure 21). Winter air temperature dominates other variables, because: 1) the high latitude of the research site results in long snow covered periods, 2) the research area is situated in the air mass boundary zone, where intermittent passages of contrasting air masses cause large fluctuations in atmospheric forcing during winter. During the summer, air temperatures are more stable, because differences in the air mass properties are subdued (Hanssen-Bauer, et al., 1990).

SPITSBERGEN AT THE AIR MASS BOUNDARY ZONE

In this section, I take a more regional view and argue that a) permafrost temperatures in Spitsbergen are dictated by atmospheric circulation, and b) because Spitsbergen is located in the Arctic air mass boundary zone, the climatic change there related to global warming may challenge our expectations of gradual high latitude warming.

In the preceding section, I showed that the mean cold season air temperature has the dominant influence on year to year variations in permafrost temperatures in western Spitsbergen. This dominance arises from both the extensive duration of the cold period and the large contemporary year to year variability in cold season air temperature, which in Spitsbergen is controlled by the contrasting dry, cold Arctic and moist, warm Atlantic air masses (Wendland and Bryson, 1981; Hanssen-Bauer et al., 1990). This is evident in a recent compilation of rawinsonde observations (1954-1990, north of 65°N), where the steepest gradient in surface temperature is located over Spitsbergen, separating the two contrasting air masses that are relatively homogeneous (figure 6b in Serreze, 1995). It can

also be seen in upper air balloon soundings from the Alfred Wegener Institute research station in Ny Alesund, that show the characteristic cold (warm) temperature profile (Figure 1) of air masses originating from the Arctic (Atlantic) ocean (Figure 2). Such an atmospheric transition zone is interpreted by Wendland and Bryson (1981) as a climatic front, defined as "...a narrow zone of transition between air masses of contrasting density, that is, air masses of different temperatures or different water vapor concentrations or both" (Moran and Morgan, 1989). The average winter air temperature at the field site is determined by the temporal contribution of both air masses; correspondingly mean winter air temperature and permafrost temperatures are both dictated by air mass circulation patterns that shift air mass boundaries.

I now turn my attention to the climatic conditions that lead to rain-on-snow events in Spitsbergen. As evident from maps of northern hemisphere daily mean sea level air pressure, anomalous pressure fields –deep low pressure over Greenland and high pressure over White Sea region– were related to each of the three rain-on-snow events recorded in 1985/86. I determined the average locations for both pressure centers, the low in Greenland (68°N, 31°W) and the high over the White Sea (64°N, 35°E). M. Serreze (pers. comm., 4/20/1997) from National Climate Data Center, computed daily pressure time series for these two locations (the original sea level pressure fields from NCEP reanalysis are provided on a 2.5 x 2.5 degree grid; to get the pressure values at the desired points a Cressman weight interpolation scheme was used, employing a 250 km search radius (pers. comm. M. Serreze, 1997)). A time series of the pressure difference between the

White Sea and Greenland was then obtained and compared to the air temperature and precipitation record for the 1985/86 winter in Ny Alesund. A pressure difference of approximately 40 mb appears to constitute a threshold above which rain fell or was most probable in western Spitsbergen in the 1985/86 winter and spring, and by inference also during the snow cover season of other years (Figure 22). This relation between the synoptic scale pressure field and weather anomalies in western Spitsbergen reflects the tendency for air masses in the northern hemisphere to circulate clockwise around high pressure centers and counterclockwise around low pressure centers. As the high is situated over the White Sea and the low over Greenland, air masses heading east are naturally forced to the north towards Spitsbergen. The strength of the air flow is related to the pressure gradient between the centers. Thus, both mean winter air temperature and number of slushlike events are dictated by circulation dynamics.

To test the general applicability of this hypothesis and possible temporal trends, these daily mean sea level pressures data set over a period of 1973-1995, were compared to climate data from the Ny Alesund research station. Peaks in this pressure index are well correlated (78 %) with winter rain events evident in meteorological records from Ny Alesund for January-March 1983-1990. The winter mean air temperature in Ny Alesund during the same period is correlated to the number of days of extreme pressure gradient ($r^2 = 0.52$). The air temperature record (unlike precipitation) extends from 1973 to 1990, and the corresponding correlation for that period is 0.52, using a 2-year running mean for both data series; using a 3-year running mean yields an r^2 of 0.83 (Figure 23). This

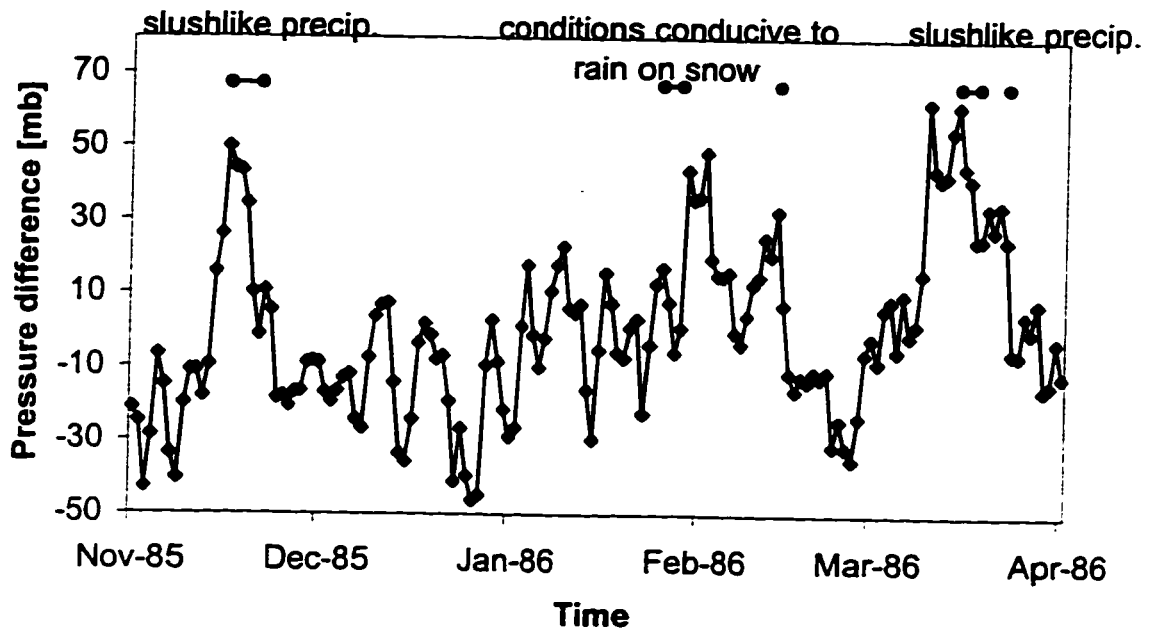


Figure 22: Winter 1985/86 sea level atmospheric pressure difference between the White Sea and Greenland (WS-G). The pressure difference related to the three distinct warming episodes exceeded 40 mb. Rain on snow was reported in the research station during two of these occasions, during the third the slush was not reported but is very likely to have occurred, based on the reported continuous precipitation and maximum air temperature reaching 2°C above freezing point. Moreover, this was the only period when these conditions prevailed outside the reported slush events. Reported and inferred periods of slush at the research station are also shown.

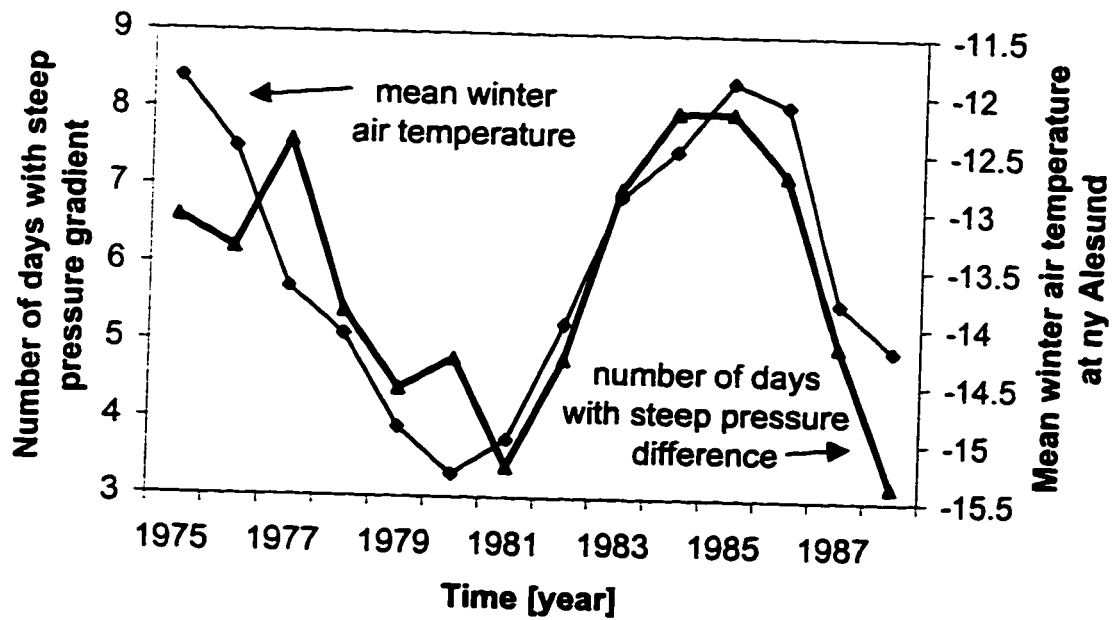


Figure 23: Five year running mean of mean winter air temperature at the Ny Alesund research station and number of days with pressure gradient >40 mb between Greenland and the White Sea in a winter, 1973-1990. This suggests that the two series are strongly correlated on a time scale of several years.

suggests that the two series are strongly correlated on a time scale of several years. This is consistent with the work of Overland and Turet (1994) which showed that transient eddies (e.g. short lived atmospheric disturbances like the anomalies correlated with the rain-on-snow events) contribute most of the atmospheric energy flux into the Arctic, through the pathway between Greenland and Scandinavia. In conclusion, I suggest that in winter, anomalously strong atmospheric flow brings relatively warm and moist air over Spitsbergen, and in extreme cases also leads to both slushlike precipitation and rain. When weaker flow prevails, air masses are modified to intermediate temperatures, and the potential for slushlike precipitation and rain is essentially eliminated.

Global change is expected to modify air mass boundaries (Hartmann, 1995, p. 335; Bowling, 1984; Trenberth, 1995) that may either amplify or retard the general warming trend at the air mass boundary zone. Such local changes are beyond the resolution of current GCM's; they will require models capable of higher spatial resolution such as nested mesoscale models or statistical relations between large scale climate and local weather patterns (IPCC, 1996). The outcome may challenge our understanding of environmental changes in certain areas, and may confound the climatic interpretation of deep borehole temperatures. Surprising and seemingly contradictory changes may take place (Trenberth, 1995).

Air mass dynamics at the boundary zone, as described above for Spitsbergen, complicate the interpretation of permafrost thermal history in other areas as well, as discussed below for Alaska where much of the deep borehole temperature data have been obtained.

CHAPTER V: AIR MASS DYNAMICS AND PERMAFROST TEMPERATURES IN ALASKA

Starting with the first deep permafrost temperature measurements in Alaska, it has long been inferred that the climate has not been steady and that the surface thermal forcing has changed through time. This was either caused by anthropogenically induced global change or was part of natural climate variability (Lachenbruch et al., 1982). Since then it has often been suggested that deep permafrost temperatures from Alaska constitute an exceptional and direct record of surface temperatures that show early signs of anthropogenic climate warming (Osterkamp and Romanovsky, 1996). However, the initial tendency to connect permafrost temperatures simply to air temperature has been difficult to maintain, partly because there is no obvious trend of increasing air temperature that corresponds to the increasing permafrost temperatures (Osterkamp, 1993; Osterkamp and Romanovsky, 1996). Moreover, the concern with the absence of a simple trend of increasing air temperature may be misleading in this context because Alaska is located in the dynamic air mass boundary zone (Polar front), where mean winter air temperatures are dictated by the relative importance of temporal contributions of shifting air masses. In this case, they are the cold Arctic and warm Pacific air masses that pass over Alaska (Bowling, 1984; Shaw, 1988 and 1991), as the Arctic front fluctuates latitudinally (Barry, 1967). Recently the warmer winter air temperatures in Alaska have been related to changes in magnitude and location of the Aleutian Low. This

low promotes the advection of warm Pacific air into Alaska (Trenberth, 1990; Trenberth and Hurrell, 1994).

I proceed to show that in Central Alaska: 1) the mean winter air temperatures, which have a dominant effect on the annually-averaged soil heat flow, are dictated more by large scale climate dynamics than by changes in local air mass characteristics; 2) no long term temperature trend is discernible in either air mass; and 3) predicted gradual climate warming is well masked by a large interannual fluctuation of mean winter air temperatures. Hence, I propose that observed changes in permafrost temperatures are much more likely to reflect changes in circulation patterns than changes in the temperature of any air mass, and that we know very little about whether such changes in circulation patterns are to be expected as part of anthropogenically induced climate change.

The two air masses that fluctuate over Alaska in winter carry an identifiable and distinct chemical signature that is related to their respective source areas (Shaw, 1988 and 1991).

It was shown that when the air temperature was at least 15°C colder than the mean seasonal air temperature, central Alaska was bathed by Arctic air (Shaw, 1988 and 1991).

These extreme cold spells typically occur several times in a winter.

I used the daily air temperature data for the 1931-1995 period from the University of Alaska experimental station located near Fairbanks in central Alaska, at an elevation of 146 m (Climatedata, 1996) to study the effect of air mass advections on mean winter air temperature. The number and duration of cold spells changes from year to year, and greatly affect the mean winter air temperature. The mean winter air temperature is highly correlated ($r^2 = 0.67$) to the number of days of extreme cold in the November-March period. Therefore, soil temperatures in Alaska are most likely responding to changes in air mass fluctuations rather than modification of a local air mass. This result is consistent with Walsh and Chapman's (1990) finding that recent temperature changes in the Arctic are circulation induced. It is also consistent with van Loon and Rogers's (1977) conclusions: "Long-term *regional* trends of mean temperature in winter are intimately associated with changes in the frequency of circulation types. It is therefore unlikely that such temperature trends are caused *directly* by variations in atmospheric constituents and aerosol content or in insolation".

To study temporal changes in temperature I calculated mean winter temperatures for both cold and warm air masses for the periods when they were distinctively present over central Alaska. For each winter I identified cold outbreaks (air temperature at least 15°C colder than seasonal mean air temperature) and warm outbreaks (air temperature warmer than -2°C, which corresponds generally with 15°C warmer than seasonal mean temperature). These extremes represent conditions when either distinct cold Arctic or warm Pacific air mass passed over central Alaska (Shaw, 1988 and 1991). No long-term

trend was discernible in the average temperature of either the cold or warm outbreaks (Figure 24).

The current state of the art GCM's (excluding, for example, the recent suggestion to downscale GCM outputs with nested mesoscale models (Russo and Zack, 1997)) are not likely to provide much guidance for anticipating environmental changes along air mass boundary zones in the Arctic, thus leaving the following important questions unanswered in these areas: How are mean winter air temperatures expected to evolve? What type of a signal should we be looking in the permafrost temperature archive? Counterintuitive changes due to general warming have been suggested (Trenberth, 1995). Therefore the effort of acquiring early warnings of climate change through monitoring of permafrost temperatures should be geared towards climatically more predictable areas, e.g. well within air masses and away from boundary areas (Figure 25).

I suggest that permafrost temperatures from air mass boundary areas could be used to study the climate dynamics, and the potentially rapid changes there. I stress that it is essential to pay careful attention to the manner in which permafrost temperatures can be modified by changes in the active layer, seasonal snow cover and in water infiltration events, which can obscure the climatic signal.

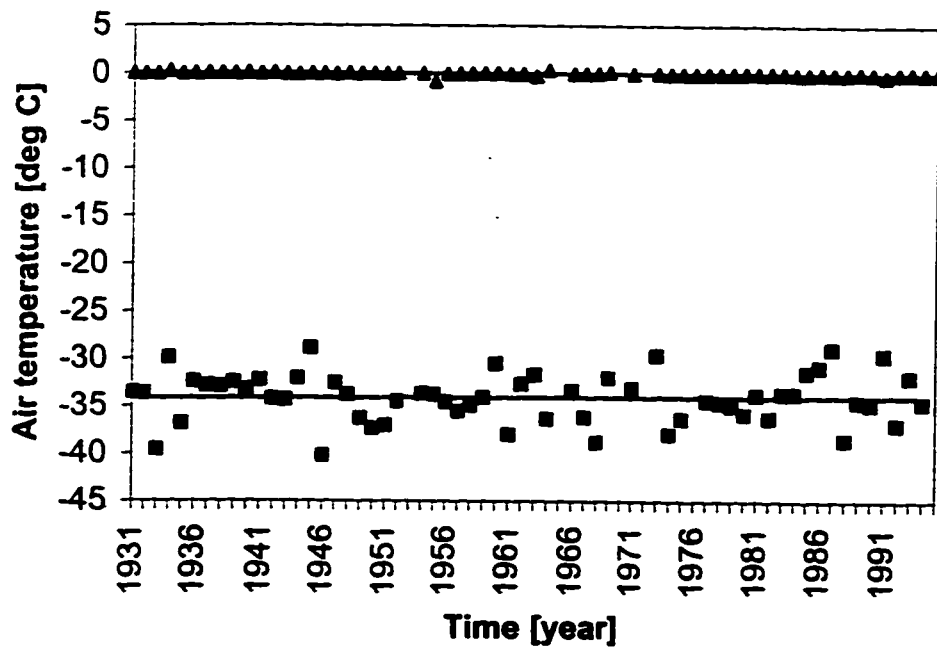


Figure 24: Mean winter temperature of cold (squares) and warm (triangles) air excursions over central Alaska, 1931-1995. Neither time series shows a warming trend.

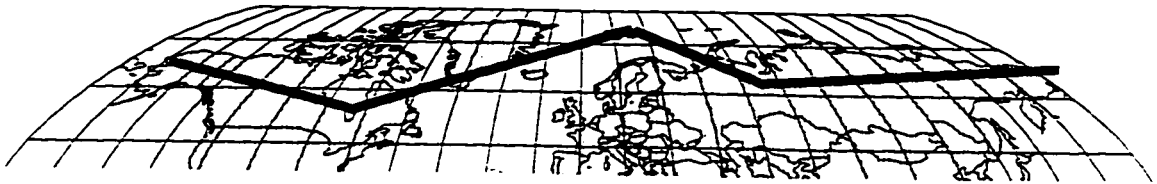


Figure 25: Location of Arctic air mass boundary (Polar front). Generalized from (Barry, 1967; Krebs and Barry, 1970)

CONCLUSIONS

The thermal link between the atmosphere and the permafrost is central to predicting climate change consequences in high latitude and high altitude areas, and to interpreting climate change records contained in permafrost temperatures. I studied this link by examining the principal atmospheric factors and heat transfer processes that dictate soil temperatures and heat flow for an Arctic desert site in western Spitsbergen (78°57'29N, 12°27'42E).

The modeling of the soil thermal regime requires a precise determination of soil thermal properties, and soil heat transfer processes. Although it is common practice to assign constant representative thermal properties to soils of interest, the thermal properties of natural soils tend to vary spatially due to changes in texture, lithology, moisture and/or organic content, and they vary with time primarily due to changes in moisture and in the relative amounts of ice and water. The one dimensional thermal conduction equation (1), contains a term explicitly accounting for the vertical thermal conductivity gradient, which is important in the energy balance for the soil at the study site, and by inference, for other natural soils. If it is omitted it leads to an apparent need to invoke processes other than conduction or thermal properties that are unrealistic. Accurate thermal modeling for laterally homogeneous soils on sub-horizontal surfaces requires in situ observations of vertically and temporally varying soil thermal properties; if thermal properties vary

laterally, accurate thermal modeling would require inclusion of the complete three-dimensional spatial variation of the thermal parameters, as well as variations in surface and other significant properties (vegetation, albedo, texture, moisture).

Water that remains unfrozen in soils at subzero temperatures, which is often neglected in soil thermal models, is important for realistic modeling of soil temperatures at the field site. During the freeze up (thaw) period, the unfrozen water dictates the typical gradual departure (approach) of temperatures from (to) 0°C. Without this term, modeled temperatures would depart abruptly from 0°C once all the water is frozen. Below approximately -3°C the effect of unfrozen water increasing the apparent heat capacity and lowering of thermal conductivity of the soil at the field site (McGaw et al., 1978) is practically negligible.

Thermal conduction is the only significant heat transfer process at this site in the soil during the summer and most of the winter. Other heat transfer processes have been invoked in other areas, but they seem unimportant in western Spitsbergen. In addition, theoretical considerations indicate that coupled energy and mass transfers contribute only insignificantly to the soil energy budget. Comparisons between modeled and observed soil temperatures are suggestive of distinct periods in the late spring when water that has become abundant in the snow percolates into and rapidly warms the frozen soil. This form of latent heat transfer amounts to 53 % of the total energy delivered to the soil during these warming periods; the rest is primarily due to heat conduction.

The soil thermal model is tied to external atmospheric forcing through air temperature during winter, and to both net radiation and air temperature during summer. During most of the winter the sun is absent at this high latitude site; the air temperature is used as a surface boundary condition. Although air temperature is commonly used as a surrogate for snow surface temperature, the daily average snow surface is up to 3.7°C colder than the air because the considerable long-wave radiation loss from the snow surface results in surface inversion. This highlights the need to either use direct measurements of snow surface temperature or to develop a transfer function between observed air temperature and snow surface temperature. Long term air temperature measurements are sparse in the high Arctic, and caution should be exercised in extrapolating these records to distant field sites. The mean air temperature for July-August, 1991 was 1.3°C lower at the field site about 2 km from the open ocean, than in Ny Alesund, about 10 km from the open ocean, and the winter 1985/86 air at the field site was 1.5°C warmer than in Ny Alesund. These differences are caused by the increased continentality in fjord interiors.

The snow cover is a dynamic link in the heat transfer from the soil to the atmosphere. The total heat flow through the snow pack depends on snow density and thickness, and on the heat transfer processes within snow pack. Typically the snow depth in the field area through most of the winter was between 1.0-1.2 m. Depth hoar is unlikely to form there due to the characteristically gentle thermal gradient in the snow pack. Moreover the

occasional rain percolating through the snow would tend to destroy the depth hoar had it formed. Heat transfer in the snow pack is essentially by conduction, except when considerable heat is delivered to the base of the snow pack, by rain infiltrating the snow cover and freezing at the soil surface. This thermally important process is absent from most snow thermal models. Its absence could partially invalidate the models that treat winter soil temperatures only as a function of air temperature and conduction through the snow pack. The most recent data set from this field site gives a preliminary indication that the thermal impact of rain-on-snow events may be considerably more important than suggested by previous data. During the 1995/96 winter the mean seasonal soil surface temperature, was over 9 °C higher than the comparable temperature during the 1985/86 reference year. This difference seems to be largely due to more frequent and longer duration rain-on-snow events in the 1995/96 winter. This is a major difference in soil surface temperature that would have been virtually missed, had the near surface temperature been calculated only as a function of air temperature with simple conduction through the snow. An increase in frequency or magnitude of such events would mimic significant air warming. Rain on snow has not been previously recognized as an important climatic forcing driving permafrost temperatures. Depending on how the occurrence and magnitude of rain-on-snow events change with the changing climate, it may turn out to be one of the strongest signals in past permafrost temperatures and one of the strongest influence of the soil thermal evolution in the future.

To assess the effects of anticipated upcoming climate change on the thermal regime of the active layer and permafrost, and to improve the interpretation of records of past soil temperatures, I determined the relative importance of atmospheric and environmental factors that control the net energy budget of high latitude soils. Contrary to common opinion, I found that probable variations in summer air temperature or radiation have little effect on the mean annual soil heat flow. The mean air temperature in the snow cover period is the single most effective determinant of mean annual soil heat flow, because of the inherently high variability of winter air temperatures and the extended duration of the snow cover period in this high latitude region. This conclusion is particularly important because of the GCM's predictions that the largest consequence of the anticipated increase in Greenhouse gases will be greatly increased winter air temperatures at high latitudes.

In a broader view, I stress two principal results. First, the onset of rapid and effective delivery of heat to the base of the snow pack by rain-on-snow events in Spitsbergen is related to an anomalously steep pressure gradient between Greenland and the White Sea. Seventy-eight percent of the rain on the snow events are correlated with extremes of this pressure gradient. Moreover the winter mean air temperature is also strongly correlated with the number of days of extreme pressure gradient, suggesting that both the mean winter air temperature and permafrost temperature are dictated by air mass circulation patterns. Second, global change is expected to impact air mass boundaries (Hartmann, 1995. p. 335., Bowling, 1984., Trenberth, 1995), which may either amplify or retard the

general warming trend at the air mass boundary zone. Local changes such as these are beyond the resolution of current GCM's, but may challenge our understanding of environmental changes in certain areas. Therefore it is important to recognize air mass boundary zones as areas where gradual climate change may be masked behind a large natural variability, as well as being areas of potentially more rapid and stronger manifestation of climate change. Nested mesoscale models as well as statistical downscaling could mitigate the resolution deficiency in the future and provide more detailed climate predictions (Russo and Zack, 1997; IPCC, 1996).

Alaska has been the locus of intense permafrost research and is also situated along an air mass boundary zone (the Polar front). Deep permafrost temperatures have been obtained from there, and it has been often suggested that they might reveal early signs of anticipated climate warming. I have shown that: 1) the mean winter air temperature in Central Alaska is likely to be dictated more by large scale climate dynamics than by changes in local air mass characteristics, 2) no long term trend is discernible in the temperature of either the Arctic or Pacific air mass and, 3) predicted gradual climate warming is well masked by a large interannual fluctuation of mean winter air temperatures that have a dominant effect on the annually-averaged soil heat flow. Hence, I propose that observed changes in permafrost temperatures are much more likely to reflect changes in circulation patterns, than changes in the temperature of any air mass. This may or may not reflect anthropogenically induced climate change.

If one wishes to study only the warming of an air mass through deep borehole temperatures, the logging site should be located well inside the air mass boundaries, for example north of Hudson Bay. I stress, however, that permafrost temperatures from sensitive air mass boundary areas (Spitsbergen, Alaska, Siberia) could be particularly useful because of their potential to record changes over tens or hundreds of years in air mass dynamics and circulation patterns (for example changes in North Atlantic Oscillation and El Nino and their effects through teleconnections at higher latitudes), well beyond the few decades for which instrumental data have become widely available.

LIST OF REFERENCES

Akitaya, E. 1974. Studies on Depth Hoar. Contributions from the Institute of Low Temperature Science, Vol. 26A, The Institute of Low Temperature Science, Hokkaido University, pp. 1-67.

Barry, R.G. 1967. Seasonal Location of the Arctic Front over North America. Geographical Bulletin, Vol. 9 (2), pp. 79-95.

Bejan, A. 1993. Heat transfer. J. Wiley & Sons, Inc. 675 p.

Berman, R.G. and T.H. Brown. 1985. Heat Capacity of Minerals in the System Na₂O-K₂O-CaO-MgO-FeO-Fe₂O₃-Al₂O₃-SiO₂-TiO₂-H₂O-CO₂: Representation, Estimation, and High Temperature Extrapolation. Contributions to Mineralogy and Petrology, Vol. 89, pp. 168-183.

Bowers, J.D. and W.G. Bailey. 1989. Summer Energy Balance Regimes for Alpine Tundra, Plateau Mountain, Alberta, Canada. Arctic and Alpine Research. Vol. 21 (2), pp. 135-143.

Bowling, S.A. 1984. The Variability of the Present Climate of Interior Alaska. In J.H. McBeath (ed.) Proceedings of a Conference: the potential effects of carbon dioxide-induced climatic changes in Alaska. pp. 67-74.

Bradley, R.S. and P.D. Jones. 1993. 'Little Ice Age' Summer Temperature Variations: Their Nature and Relevance to Recent Global Warming Trends. *The Holocene* 3(4), pp. 367-376.

Bryson, R.A. 1966. Air Masses, Streamlines, and the Boreal Forest. *Geographical Bulletin*, Vol. 8 (3), pp. 228-269.

Budyko, M.I. and Y.A. Izrael. 1987. Anthropogenic Climatic Change. 405 p. Hydrometeoizdat, Leningrad, in Russian; English edition published by the University of Arizona press 1992.

Carsel, R.F. and R.S. Parrish. 1988. Developing Joint Probability Distributions of Soil Water Retention Characteristics. *Water Resources Research*, Vol. 24 (5), pp. 755-769.

Chamberlain, E.D. and A.J. Gow. 1979. Effect of Freezing and Thawing on the Permeability and Structure of Soils. In: *Ground Freezing*, Jessberger, H.L. (ed). *Engineering Geology*, Vol. 13, (1-4), pp. 73-92.

Chapman, W.L. and J.E. Walsh. 1993. Recent Variations of Sea Ice and Air Temperature in High Latitudes. *Bulletin of American Meteorological Society*, Vol. 74, pp. 33-47.

Clark, S.P. 1966. Thermal conductivity in *Handbook of Physical Constants: Memoir 97*, S.P. Clark, Editor. Geological Society of America, New York, pp. 459-482.

Climatedata. 1996. Climatedata NCDC summary of the day [computer file]. Hydrosphere Data Products, Boulder, Colorado.

Colbeck, C.S. 1983. Ice Crystal Morphology and Growth Rates at Low Supersaturations and High Temperatures. *Journal of Applied Physics*. Vol. 54, pp. 2677-2682.

Dozier, J. and S.G. Warren. 1982. Effect of Viewing Angle on the Infrared Brightness Temperature of Snow. *Water Resources Research*, Vol. 18, (5), pp. 1424-1434.

Dunne, T. and L.B. Leopold. 1978. *Water in Environmental Planning*. Freeman and Company, New York. 818 p.

Etzelmuller, B. and J.L. Sollid. 1991. The role of weathering and pedological processes for the development of sorted circles on Kvadehuksletta, Svalbard – a short report. *Polar Research*, Vol. 9 (2), pp. 181-191.

Goodison, B.E., H.L. Ferguson and G.A. McKay. 1981. Measurement and Data Analysis, in Handbook of Snow, Gray, D.M., and D.H. Male (eds.). Pergamon Press. 650 p.

Goodrich, L.E. 1982. The Influence of Snow Cover on the Ground Thermal Regime. Canadian Geotechnical Journal Vol. 19, pp. 421-432.

Gregersen, O. and T. Eidsmoen. 1988. Permafrost Conditions in the Shore Area at Svalbard. Fifth International Conference on Permafrost in Trondheim, Norway, August 1988. Vol. 2, pp. 933-936.

Grey, J.M.N.T, G.L.W. Morland and S.C. Colbeck. 1995. The Effect of Change in Thermal Properties on the Propagation of a Periodic Thermal Wave: Application to a Snow Buried Rocky Outcrop. Journal of Geophysical Research, Vol. 100 (B8), pp. 15,267-15,279.

Gunn, K.L.S. 1965. Measurements on New Fallen-Snow. Stormy Weather Group Scientific Report MW-44, McGill University, Montreal, Canada, 25 p.

Hagen, J.O. and O. Liestol. 1990. Long-Term Glacier Mass-Balance Investigations in Svalbard. Annals of Glaciology. Vol 14.

Hagen, J.O., O. Liestol, Roland and Jorgensen. 1993. Glacier Atlas of Svalbard and Jan Mayen. Norsk Polarinstitut Meddelelser 129.

Hallet, B. and Prestrud, S. 1986. Dynamics of Periglacial Sorted Circles in Western Spitsbergen. *Quaternary Research*, Vol. 26, pp. 81-99.

Hallet, B. and Rasmussen, A. 1993. Calculation of the Thermal Conductivity of Unsaturated Frozen Soil near the Melting Point. *Permafrost sixth International Conference Proc.* Vol. 1, pp. 226-231. South China University of Technology Press.

Hanssen-Bauer, I., M. Kristensen Solas and E.L. Steffensen. 1990. The Climate of Spitsbergen. Rapport Nr. 39/90. Det Norske Meteorologiske Institutt. 40 p.

Hartmann, D.L. 1994. *Global Physical Climatology*. Academic Press, Inc. 411 p.

Hinkel, K.M. and S.I. Outcalt. 1993. Detection of Nonconductive Heat Transport in Soils Using Spectral Analysis. *Water Resources Research*, Vol. 29, (4), pp. 1017-1023.

Hinkel, K.M. and S.I. Outcalt. 1994. Identification of Heat-Transfer Processes during Soil Cooling, Freezing, and Thaw in Central Alaska. *Permafrost and Periglacial Processes*, Vol. 5, pp. 217-235.

Hinkel, K.M., S.I. Outcalt and F.E. Nelson. 1990. Temperature Variation and Apparent Thermal Diffusivity in the Refreezing Active Layer, Toolik Lake, Alaska. *Permafrost and Periglacial Processes*, Vol. 1, pp. 265-274.

Hisdal, V., O. Finnekasa and T. Vinje. 1992. Radiation Measurements in Ny-Alesund, Spitsbergen 1981-1987. Norsk Polarinstitutt, Oslo. Meddelelser Nr. 118. 380 p.

IPCC. 1990. (Intergovernmental Panel on Climate Change). Seasonal snow cover, ice and permafrost. In *Potential Impacts of Climate Change*, IPCC, Report for Working Group 2, Sections 7.1-7.45.

IPCC. 1996. (Intergovernmental Panel on Climate Change). *Climate Change 1995, The Science of Climate Change*. Cambridge University Press. 572 p.

Isard, S.A. and M.J. Belding. 1989. Evapotranspiration from the Alpine Tundra of Colorado, U.S.A. *Arctic and Alpine Research*, Vol. 21 (1), pp. 71-82.

Johansen, O. 1975. *Thermal Conductivity of Soils*. Ph.D. thesis, Trondheim, Norway. (CRREL Draft Translation 637, 1977). ADA 044002.

Jordan, R. 1991. *A One-Dimensional Temperature Model for a Snow Cover*. Cold Regions Research and Engineering Laboratory, Special Report.

Judge, A. and J. Pilon. 1984. **Climate Change and Geothermal Regime**. Introduction in **Fourth International Conference on Permafrost, Final Proceedings**, National Academy Press, US. pp. 137-138.

Kahl, J.D., D.J. Charlevoix, N.A. Zaltseva, R.C. Schnell and M.C. Serreze. 1993. **Absence of Evidence for Greenhouse Warming over the Arctic Ocean in the Past 40 Years**. *Nature*, Vol. 361 (6410), pp. 335-337.

Kane, D.L., L.D. Hinzman and J.P. Zarling. 1991. **Thermal Response of the Active Layer to Climatic Warming in a Permafrost Environment**. *Cold Regions Science and Technology*, Vol. 19 (2), pp. 111-122.

Koenig-Langlo, G. and Marx, B. 1997. **The Meteorological Information System at the Alfred Wegener Institute**. In: **Climate and Environmental Database Systems**. Edited by Lautenschlager, M. and Reinke, M. Kluwer Academic Publisher. Printed in USA Norwell.

Kojima, K. 1967. **Densification of Seasonal Snow Layers**. *Physics of Snow and Ice, Proceedings of International Conference on Low Temperature Science, Sapporo*, pp. 929-952.

Krebs, J.S. and R.G. Barry. 1970. The Arctic Front and the Tundra-Taiga Boundary in Eurasia. *The Geographical Review*. pp. 548-554.

Lachenbruch, A.H. and B.V. Marshall. 1986. Changing Climate: Geothermal Evidence from Permafrost in the Alaskan Arctic. *Science*, Vol. 234, pp. 689-696.

Lachenbruch, A.H., J.H. Sass, B.V. Marshall and T.H. Moses, Jr. 1982. Permafrost, Heat Flow, and the Geothermal Regime at Prudhoe Bay, Alaska. *Journal of Geophysical Research*. Vol. 87 (B11), pp. 9301-9316.

Liestol, O. 1975. Glaciological Work in 1972. *Norsk Polarinstitutt Arbok 1972*, pp. 125-135.

Mackay, J.R. 1983. Downward water movement into frozen ground, western arctic coast, Canada. *Canadian Journal of Earth Sciences*. Vol. 20 (1), pp. 120-134.

Mann, D.H., R.S. Sletten and F.C. Ugolini. 1986. Soil Development at Kongsfjorden, Spitsbergen. *Polar Research*, Vol. 4. Pp. 1-16.

Marbouty, D. 1980. An Experimental Study of Temperature-Gradient Metamorphism. *Journal of Glaciology*. Vol. 26 (94), pp. 303-312.

Marsh, P. and M. Woo. 1984. Wetting Front Advance and Freezing of Meltwater Within a Snow Cover 1. Observations in the Canadian Arctic. *Water Resources Research*, Vol. 20 (12), pp. 1853-1864.

Marsh, P. and M. Woo. 1984. Wetting Front Advance and Freezing of Meltwater Within a Snow Cover 2. A Simulation Model. *Water Resources Research*, Vol 20 (12), pp. 1865-1874.

Maxwell, J.B. and L.A. Barrie. 1989. Atmospheric and Climatic Change in the Arctic and Antarctic. *Ambio* Vol. 1, pp. 42-49.

McGaw, R.W., S.I. Outcalt and E. Ng. 1978. Thermal Properties and Regime of Wet Tundra Soils at Barrow, Alaska. *Third International Conference on Permafrost, Proceedings*, Vol 1. July 10-13, 1978, Edmonton, Alberta, Canada. National Research Council of Canada. pp. 47.

Meehl, G.A., W.M. Washington, D.J. Erickson III, B.P. Briegleb and P.J. Jaumann. 1996. Climate Change from Increased CO₂ and Direct and Indirect Effects of Sulfate Aerosols. *Geophysical Research Letters*, Vol. 23 (25), pp. 3755-3758.

Mellor, M. 1964. Properties of Snow. Cold Regions Research and Engineering Laboratory, Cold Regions Science and Engineering Monograph III-AI. AD611023.

Mietus, M. 1991. Snow depth at the Hornsund Station, Spitsbergen in 1978-1986. Polish Polar Research. Vol. 12 (2), pp. 223-228.

Milly, P.C.D. 1982. A Simulation Analysis of Thermal Effects on Evaporation From Soil. Water Resources Research, Vol. 20 (8), pp. 1087-1098.

Moran, J.M. and M.D. Morgan. 1989. Meteorology, the Atmosphere and the Science of Weather. 2nd edition. Macmillan Publishing Company. New York. 557 p.

Nelson, F.E., A.H. Lachenbruch, M.-k. Woo, E.A. Koster, T.E. Osterkamp, M.K. Gavrilova, C. Guodong. 1993. Permafrost and Changing Climate. Sixth International Conference on Permafrost. South China University of Technology, Wushan Guangzhou, China.. Presentation by the authors in a plenary session on "Global Climate Change and Permafrost".

Nelson. F.E. and O.A. Anisimov. 1993. Permafrost Zonation in Russia under Anthropogenic Climatic Change. Permafrost and Periglacial Processes, Vol. 4 (3), pp. 137-148.

Oechel, W.C., S.J. Hastings, G.V. Vourlitis, M. Jenkins, G. Riechers and N. Grulke. 1993. Recent Change of Arctic Tundra Ecosystems from a Net Carbon Dioxide Sink to a Source. *Nature*, Vol. 361, pp. 520-523.

Osterkamp, T.E. and J.P. Gosink. 1991. Variations in Permafrost Thickness in Response to Changes in Paleoclimate. *Journal of Geophysical Research*, Vol. 96 (B3), pp. 4423-4434. American Geophysical Union.

Osterkamp, T.E. and V.E. Romanovsky. 1996. Characteristics of changing permafrost temperatures in the Alaskan Arctic, USA. *Arctic and Alpine Research*. Vol. 28 (3), pp. 267-273.

Overland, J.E and P. Turet. 1994. Variability of Atmospheric Energy Flux Across 70N: Computed from the GFDL data set. In: *Nansen Centennial Volume*, O. Johannessen, R. Muench and J. Overland, Editors, American Geophysical Union.

Ozisik, M.N. 1968. *Boundary Value Problems of Heat Conduction*. Dover Publications, Inc. 504 p.

Pavlov, A.V. 1996. Permafrost-Climatic Monitoring of Russia: Analysis of Field Data and Forecast. *Polar Geography and Geology*. Vol. 20 (1), pp. 44-64.

Permafrost Research. 1983. *An Assessment of Future Needs*. Committee on Permafrost, Polar Research Board, National Research Council. National Academy Press, Washington, D.C. 103 p.

Philip. J.R. and D.A. de Vries. 1957. *Moisture Movement in Porous Materials under Temperature Gradients*. Transactions, American Geophysical Union. Vol. 38 (2), pp. 222-232.

Richtmeyer, R.D. and Morton, K.W. 1967. *Difference Methods for Initial Value Problems*. J.Wiley & Sons.

Rind, D.H. and J.T. Overpeck. 1995. *Modeling the Possible Causes of Decadal-to-Millennial-Scale Variability*. Natural Climate Variability on Decade-to-Century Time Scales, National Research Council. pp. 187-217.

Riseborough, D.W. and M.W. Smith. 1993. *Modeling Permafrost Response to Climate Change and Climate Variability*. in Lunardini, V.J. and S.L. Bowen, (eds.) Proceedings, Fourth International Symposium on Thermal Engineering & Science for Cold Regions, pp. 179-187. US Army Cold Regions Research and Engineering Laboratory, Special Report 93-22, Hanover, NH.

Romanovsky, V.E. and T.E. Osterkamp. 1995. Interannual Variations of the Thermal Regime of the Active Layer and Near-Surface Permafrost in Northern Alaska. *Permafrost and Periglacial Processes*, Vol. 6, pp. 313-335.

Roots, E.F. 1989. Climate Change: High Latitude Regions. *Climatic Change*, Vol. 15 (1/2), pp. 223-253.

Rott, H. and F. Obleitner. 1992. The Energy Balance of Dry Tundra in West Greenland. *Arctic and Alpine Research*, Vol. 24 (4), pp. 352-362.

Rouse, W.R. 1984. Microclimate at Arctic Treeline. 2. Soil Microclimate of Tundra and Forest. *Water Resources Research*, Vol. 20, pp. 67-73.

Rouse, W.R., S. Hardill and P.M. Lafleur. 1987. The Energy Balance in The Coastal Environment of James Bay and Hudson Bay during the Growing Season. *Journal of Climatology*, Vol. 7, pp. 165-179.

Russo, J.M. and J.W. Zack. 1997. Downscaling GCM Output with a Mesoscale Model. *Journal of Environmental Management*, Vol. 49, pp. 19-29.

Santer, B.D., K.E. Taylor, T.M.L. Wigley, J.E. Penner, P.D. Jones and U. Cubasch. 1995. Towards the Detection and Attribution of an Anthropogenic Effect on Climate. *Climate Dynamics*, Vol. 12, pp. 77-100.

Sass, J.H., A.H. Lachenbruch and R.J. Munroe. 1971. Thermal Conductivity of Rocks from Measurements of Fragments and Its Application to Heat-Flow Determinations. *Journal of Geophysical Research*, Vol. 76 (14), pp. 3391-3401.

Scanlon, B.R. and P.C.D. Milly. 1994. Water and Heat Fluxes in Desert Soils 2. Numerical Simulations. *Water Resources Research*, Vol. 30 (3), pp. 721-733.

Schmitt, E. 1993. Global Climate Change and Some Possible Geomorphological and Ecological Effects in Arctic Permafrost Environments, Isfjorden and Liefdefjorden, Northern Spitsbergen. *Permafrost sixth International Conference Proc. Vol. 1*. South China University of Technology Press. pp. 544-549.

Schwartz, M.D. and B.R. Skeeter. 1994. Linking Air Mass Analysis to Daily and Monthly Mid-Tropospheric Flow Patterns. *International Journal of Climatology*, Vol. 14, pp. 439-464.

Seligman, G. 1980. *Snow Structure and Ski Fields*. International Glaciological Society Cambridge CB2 1ER, England.

Serreze, M.C., M.C. Rehder, R.G. Barry, J.D. Kahl and N.A. Zaitseva. 1995. The Distribution and Transport of Atmospheric Water Vapor over the Arctic Basin. *International Journal of Climatology*, Vol. 15 (7), pp. 709-727.

Shaw, G.E. 1988. Chemical Air Mass Systems in Alaska. *Atmospheric Environment*, Vol. 22 (10), pp. 2239-2248.

Shaw, G.E. 1991. Aerosol Chemical Components in Alaska Air Masses 1. Aged Pollution. *Journal of Geophysical Research*, Vol. 96 (D12), pp. 22,357-22,368.

Shiozawa, S. and G.S. Campbell. 1990. Soil Thermal Conductivity. *Remote Sensing Reviews*, Vol. 5 (1), pp. 301-310.

Spencer, R.W. 1994. Global Temperature Monitoring from Space. *Advances in Space Research*, Vol 14 (1), pp. 69-75.

Sturm, M. and J.B. Johnson. 1991. Natural Convection in the Subarctic Snow Cover. *Journal of Geophysical Research*, Vol. 96 (B7), pp. 11,657-11671.

Sturm, M., J Holmgren and G.E. Liston. 1995. A Seasonal Snow Cover Classification System for Local to Global Applications. *Journal of Climate*, Vol. 8 (5), pp. 1261-1283.

Sturm, M., J Holmgren, M. Konig, K. Morris. 1996. The Thermal Conductivity of Seasonal Snow. Submitted to Journal of Glaciology.

Tao, X., J.E. Walsh, and W.L. Chapman. 1996. An assessment of Global Climate Model Simulations of Arctic Air Temperatures. Journal of Climate. Vol 9, pp. 1060-1076

Trabant, D. and C. Benson. 1972. Field Experiments on the Development of Depth Hoar. Geological Society of America, Memoir 135.

Trenberth, K.E. 1990. Recent Observed Interdecadal Climate Changes in the Northern Hemisphere. Bulletin of American Meteorological Society. Vol 71, pp. 988-993.

Trenberth, K.E., and J.W. Hurrell. 1994. Decadal Atmosphere-Ocean Variations in the Pacific. Climate Dynamics, Vol 9, pp. 303-319.

Trenberth, K.E. 1995. Atmospheric Circulation Climate Changes. Climatic Change. Vol 31, pp. 427-453.

van Genuchten, M.Th. 1976. A Closed Form Equation for Predicting the Hydraulic Conductivity of Unsaturated Soils. Soil Science Society of America Journal, Vol. 44.

van Loon, H. and J. Williams. 1976. The Connection Between Trends of Mean Temperature and Circulation at the Surface: Part I. Winter. *Monthly Weather Review*, American Meteorological Society, Vol. 104

van Loon, H. and J.C. Rogers. 1978. The Seesaw in Winter Temperatures between Greenland and Northern Europe. Part I: General Description. *Monthly Weather Review*, American Meteorological Society, Vol. 106, pp. 296-310.

Walsh, J.E. 1993. The Elusive Arctic Warming. *Nature* Vol. 361 (6410), pp. 300-301.

Walsh, J.E. and W.L. Chapman. 1990. Short-Term Climatic Variability of the Arctic. *Journal of Climate*, American Meteorological Society, Vol. 3, pp. 237-250.

Weick, E.J., and W.R. Rouse. 1991. Advection in the Coastal Hudson Bay Lowlands, Canada. I. Terrestrial Surface Energy Balance. *Arctic and Alpine Research*, Vol. 23 (3). pp. 328-337.

Weller, G. and B. Holmgren. 1974. The Microclimates of the Arctic Tundra. *Journal of Applied Meteorology*, Vol. 13, pp. 854-862.

Wendland, W.M. and R.A. Bryson. 1981. Northern Hemisphere Airstream Regions. *Monthly Weather Review*, American Meteorological Society, Vol. 109, pp. 255-270.

Williams, P.J., and M.W. Smith. 1989. *The Frozen Earth, Fundamentals of Geocryology. Studies in Polar Research.* Cambridge University Press. 306 p.

Woo, M. and R. Heron. 1981. Occurrence of Ice Layers at the Base of High Arctic Snowpacks. *Arctic and Alpine Research*, Vol. 13 (2), pp. 225-230.

Woo, M., R. Heron and P. Marsh. 1981. Basal Ice Layers of Very Cold Arctic Snowpacks. *Proceedings of the Eastern Snow Conference, 38 Annual Meeting, Syracuse, N.Y. June 4-5, 1981.*

Woo, M. and Z. Xia. 1996. Effects of Hydrology on the Thermal Conditions of the Active Layer. *Nordic Hydrology*, Vol. 27, pp. 129-142.

Yamazaki, T., J. Kondo, T. Sakuraoka and T. Nakamura. 1993. A One-Dimensional Model of the Evolution of Snow-Cover Characteristics. *Annals of Glaciology*. Vol 18, pp. 22-26.

Yen, Y. 1981. *Review of Thermal Properties of Snow, Ice and Sea Ice.* Cold Regions Research and Engineering Laboratory report 81-10.

Zhang, T. and T.E. Osterkamp. 1993. **Changing Climate and Permafrost Temperatures in the Alaskan Arctic. In Proceedings of the sixth International Conference on Permafrost, Volume 1, pp. 783-788. South China University of Technology Press, Wushan Guangzhou, China.**

Zhang, T., T.E. Osterkamp and K. Stamnes. 1996. **Influence of the depth hoar layer of the seasonal snow cover on the ground thermal regime. Water Resources Research, Vol 32 (7), pp. 2075-2086.**

APPENDIX A: FINITE DIFFERENCE DISCRETIZATION

A frequently used and readily applicable method in the numerical solution of differential equations is the finite-difference approximation of the partial derivatives (Ozisik, 1968; Richtmeyer and Morton, 1967; Bejan, 1993). The one dimensional transient diffusion of heat is described by equation (1.1)

$$\rho c \frac{\partial T}{\partial t} = \frac{\partial}{\partial z} \left(k \frac{\partial T}{\partial z} \right) \quad (1.1)$$

where T is temperature [$^{\circ}\text{C}$], t is time [s], ρc is heat capacity [$\text{J m}^{-3} \text{K}^{-1}$], k is thermal conductivity [$\text{W m}^{-1} \text{K}^{-1}$], z is depth [m].

The explicit forward discretization of equation (1.1) is represented by equation (1.2)

$$\rho c \frac{T_i^{n+1} - T_i^n}{\Delta t} = \left[k_{i-1} \left(\frac{T_{i-1}^n - T_i^n}{\Delta x} \right) - k_i \left(\frac{T_i^n - T_{i+1}^n}{\Delta x} \right) \right] \frac{1}{\Delta x} \quad (1.2)$$

where n indicates the time step and i represents equally spaced nodes along the z-axis.

The solution will be numerically stable if (Ozisik, 1968; Richtmeyer and Morton, 1967):

$$\frac{\left(2 \frac{k}{\rho c} \Delta t\right)}{(\Delta x)^2} \leq 1$$

(1.3)

This essentially defines the mesh dimensions (length and time increments).

VITA

Jaakko Kalervo Putkonen

University of Washington

1997

Master of Philosophy, 1990, University of Helsinki; Title of Masters Thesis: Permafrost Active Layer in Disko Island, Greenland.

Lovlie, R. and J.K. Putkonen. 1996. Dating of Thaw Depths in Permafrost Terrain by Paleomagnetic Method: Experimental Acquisition of a Freezing Remanent Magnetization. Geophysical Journal International, Vol. 125, pp. 850-856.

Putkonen, J.K. and B. Hallet. 1995. Importance of Vertical Variations on Thermal Properties in Modeling Heat Conduction in the Thawed Active Layer. EOS, Fall Meeting Supplement, Transactions, American Geophysical Union.

Hallet, B. and J.K. Putkonen. 1994. Surface Dating of Dynamic Landforms: Young Boulders on Aging Moraines. Science, Vol 265, pp 937-940.

Putkonen, J.K. and B. Hallet. 1994. Thermal Link Between the Atmosphere and Permafrost. EOS, Fall Meeting Supplement, Transactions, American Geophysical Union.

Putkonen, J.K. 1991. Active Layer of Permafrost. In: S. Autio (ed) Current Research 1989-1990. Geological Survey of Finland, Special Paper 12.